Detection of Salinity Changes in the North Atlantic due to the Messinian Salinity Crisis

A quantitative paleo-salinity reconstruction in the North Atlantic Ocean

By Jeroen Metz 3373673,

1st supervisor: Frits Hilgen

2nd supervisor: Maria Tulbure

Contents

1. Abstract

The Messinian salinity crisis (MSC) is the ca. 670 kyr interval wherein the Mediterranean Sea transformed into an evaporitic basin. During the MSC, more than 10^6 km^3 of evaporite was deposited in the circum-Mediterranean region, with the bulk of this volume being deposited in deep basins. The current study attempted to use an extra-Mediterranean record as an age constraint on events in the deep basins of the Mediterranean Sea, by detecting MSC related changes in paleosalinity. The proxy for paleosalinity was based on the Na/Ca ratio of *Neogloboquadrina acostaensis* test as a proxy for salinity.

Results demonstrated no significant change in Na/Ca over the interval from 5.6 to 5.3 Ma thus, the salt drawdown in the Mediterranean basin could not be detected in the paleosalinity reconstruction. This may show that halite deposition was a gradual process and the slow rate of salinity decline was below the level detectable with the Na/Ca proxy. This would refute the three-stage model of the MSC. Another explanation for this result is that the paleosalinity reconstruction failed because Na/Ca is not a suitable proxy for paleosalinity. Future research needs to investigate further whether the Na/Ca record is a reliable proxy for paleosalinity and whether the high Na/Ca pulse found in our study can be replicated. If detection of this pulse can be reproduced in another record, then it may yet be an indicator of ocean chemistry changes due to the MSC. This pulse may be correlated to the onset of stage 3 and could therefore lead to corroboration of the three-stage model.

2. Introduction

The Messinian Salinity Crisis (MSC) was an ecological event affecting the whole Mediterranean basin during the late Miocene (Figure 1). More than one million cubic kilometers of evaporite accumulated on the Mediterranean Sea-floor in deposits reaching up to 3.5 km in thickness (Roveri et al., 2014). A gradual restriction of the exchange of water between the Atlantic Ocean and the Mediterranean Sea during the MSC led to higher salinities in the Mediterranean basin. Tectonic activity in context of the convergence of the Iberian and African plates set the boundary conditions for the restriction. The timing of changes in the MSC was controlled by local isostatic processes and glacio-eustatic sea level changes (Manzi et al., 2013; Ohneiser et al., 2015).
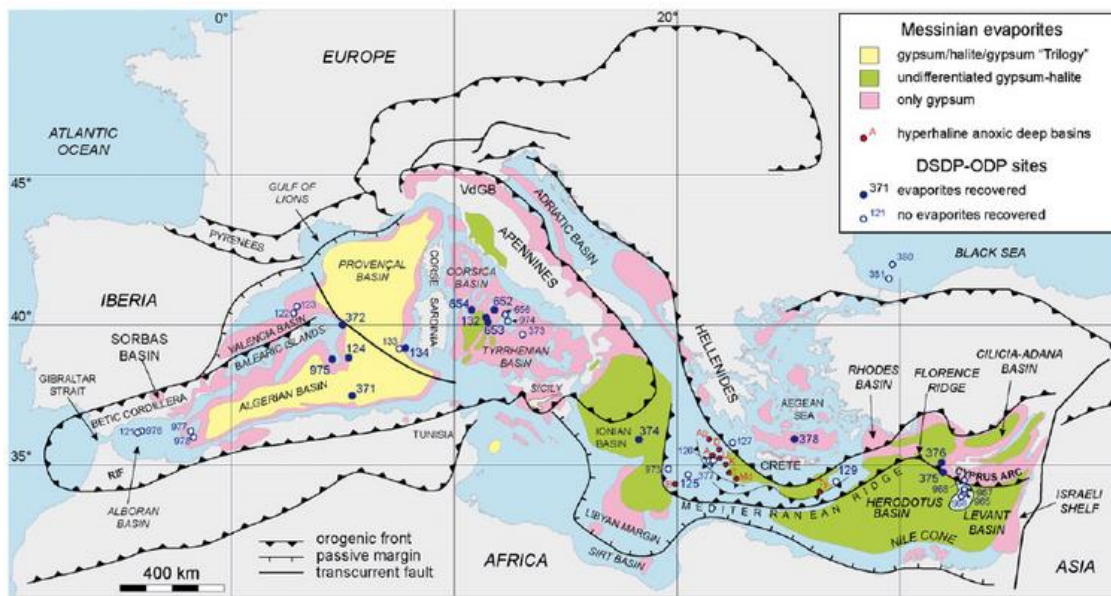

Figure 1. *A map of the Mediterranean distribution of Messinian evaporites and location of the DSDP-ODP boreholes which recovered Messinian deposits. The location of the main hyperhaline anoxic deep basins on top of the Mediterranean Ridge is also shown: Ap, Aphrodite; A, Atlante; B, Bannock; D, Discovery; K, Kryos; M, Medee; T, Thetis; Ty, Tyro; U, Urania. From Roveri et al., 2014*

2.1 Problem statement

The bulk of salt deposited during the MSC lies in the deepest parts of the Mediterranean basin. Until recently, no continuous record of the deep basin deposits had been recovered and most research has been done on uplifted and exposed on-shore records from marginal and shallow basins. The correct correlation of these records to the deep-basin setting is an open question, leaving the deep basin without independent time constraints. Records with a well-established age model that covers the whole MSC interval are available for extra-Mediterranean sites. If such a record can be linked to the record of deep Mediterranean basins, then this could provide reliable time constraints. This approach is taken in this study.

The most widely accepted frame work for the MSC is that the salinity crisis went through three stages (Roveri et al., 2014). The first stage is associated with gypsum precipitation in the peripheral basins. The second stage which saw the bulk of evaporite was deposited in the deepest parts of the Mediterranean, over a brief interval of 50kyr. The final third stage saw evaporite precipitation continue in some parts of the basin, but other parts had a brackish water environment and fauna with strong links to the Paratethian When the Atlantic gateway was reopened in the Zanclean flood, the normal sea hydrology was reestablished.

The short stage 2 interpretation is based on limited evidence from the marginal settings (Roveri et al., 2014); however, if this interpretation is correct then the rapid draw down of halite would have lowered the salinity of the open oceans (Ryan et al., 2009). Salinity can thus provide the link between the deep basins in the Mediterranean and the wider ocean system. Therefore, the following central research question is formulated:

How can a North Atlantic marine record give time constraints for the Mediterranean deep-basin setting during the MSC?

To answer the research question two hypotheses have been formulated. The first hypothesis is that:

The paleosalinity reconstructed for the North Atlantic will show a decline over the course of the MSC.

With this hypothesis the groundwork for a link between North Atlantic salinity and Mediterranean events in the MSC has been established. Then during the acme of deposition, the drawdown should be greatest and thus the rate of salinity decline in the North Atlantic should also be greatest in stage two. A second hypothesis can be formulated.

The rate of salinity decline was greater over stage 2 of the MSC than in either of the other stages.

If both hypotheses are correct, then the age model of ODP core 982 can be used to constrain the beginning and end of stage two of the MSC, with its rapid deposition of evaporite in the deep basins.

3. Background

The MSC has been an object of intense interest to geo and marine science since the first inclinations of large scale evaporite deposition (Selli, 1954 cited by Roveri et al., 2014; Ryan et al., 1976). Small seas transforming into large evaporitic basins have been a recurring feature of the Earth's past, but at present no body of water of such a scale exists (Waren, 2010). The Mediterranean offers a unique chance to study a large evaporitic basin, as it is the most recent such basin and its features are relatively undisturbed (Roveri et al., 2014).

The North Atlantic-Mediterranean gateway has great influence on the Mediterranean ecology, because more water evaporates from the Mediterranean Sea than it gains from fluvial inputs and precipitation. The hydrological budget of the Mediterranean area is balanced by an inflow of water from

the North Atlantic Ocean at the Gibraltar Strait (Soto-Navarro et al., 2010). Currently the Mediterranean salinity budget is also balanced by an outflow of relatively saline water from the Mediterranean Sea.

During the MSC, the salinity in the Mediterranean basin must have been elevated so that evaporite deposition could occur. To elevate the salinity levels, the North Atlantic-Mediterranean gateway must have been restricted and the outflow of Mediterranean water severely limited. To precipitate the observed volume of evaporite observed in the Mediterranean basin, some level of inflow from the North Atlantic must have been sustained (Warren, 2010; Roveri et a., 2014). Thus the configuration of the Mediterranean-Atlantic gateway over the MSC was a key feature for the situation of the Mediterranean Sea.

3.1 Geological setting

In the Messinian, the Mediterranean gateway with the North Atlantic Ocean was located on the western edge of the basin (Flecker et al., 2015; Duggen et al., 2003). The restriction of this gateway began long before the basin wide precipitation of evaporites in the Mediterranean basin. A decline in paleo-environmental conditions started at 7.25 Ma, which is the first sign for gateway restriction. This is how the base of the Messinian was defined within the Mediterranean basin (Selli, 1960 cited by Hilgen et al., 2000; Kouwenhoven et al., 2003). To expand the definition for the Messinian to extra-Mediterranean sites, the first regular occurrence of *Globorotalia miotumida* and the first occurrence of *Amaurolithus delicatus* was set as the Global Boundary Stratotype Section and Point for the Messinian (Hilgen et al. 2000). At 6.7 Ma the diversity of calcareous plankton in the Mediterranean was suddenly reduced, which is associated with a rise in salinity and water stratification (Sierro et al. 2003). After ca. 6.3 Ma there were hypersaline events which involved the complete disappearance of planktonic foraminifera (Blanc-Valleron et al., 2002). The restriction of the gateway was a slow acting process which gradually reduced the connectivity between the Mediterranean Sea and the North Atlantic over more than a million years.

During the Messinian, the North Atlantic gateway was not always sited in the same position. Before 6.18 Ma the Betic gateway, in modern day Spain, was the main connection with the North Atlantic Ocean (Flecker et al., 2015). The position of the gateway during the MSC is not certain (Tulbure et al. 2017). Terrestrial fauna exchanges between Iberia and North Africa around 6.2 Ma (Gibert et al., 2013; García-Alix et al., 2016) and between 5.5 and 5.3 Ma (Agustí et al., 2006) indicate that the gateway was episodically closed or very shallow. An inflow of salt from the North Atlantic into the Mediterranean is required to precipitate the observed volume of evaporites. Krijgsman & Meijer (2008) showed that sufficient inflow form the North Atlantic Ocean could have been achieved with the episodic opening of a shallow gateway. The gateway must have remained restricted throughout the whole Messinian, because no precipitation would have occurred if there had been a Mediterranean outflow.

Tectonic activity set the background conditions for the restriction of the gateway (Flecker et al., 2015). On the western edge of the Mediterranean basin, the African plate converged with the Iberian plate, which caused uplift (Duggen et al., 2003). It should be noted that phases of convergence and uplift were alternated by phases of extension and subsidence due to the combination with slab rollback (Flecker et al., 2015) and the westward motion of the Alborán Domain (Duggen et al., 2004). Regionally, a component of the uplift was likely due to asthenosphere upwelling and lithospheric delamination.

Isostatic loading and unloading was another factor that caused uplift and subsidence at the gateway (Govers et al., 2009). Large scale evaporite deposition resulted in lithospheric flexure that

caused subsidence in the depocenters and uplift at the margins. Conversely, sea level fall within the Mediterranean basin resulted in unloading, which caused uplift in the depocenters and subsidence on the margins. These feedback loops were another factor in the configuration of the Atlantic gateway (Govers et al., 2009; Ohneiser et al., 2015). The elevated and exposed nature made of any barrier in the gateway made it susceptible to erosion. This makes it unlikely that the features of these barriers would have been preserved, which means that it may be impossible to determine the exact configuration of the gateway during the MSC (Flecker et al., 2015).

The timing of gateway restriction indicates that climatic processes with an astronomically forced period controlled the timing of the gateway restriction and thereby the rate of precipitation in the Mediterranean basin during the MSC (Hilgen et al., 2007). Since sea-level changes are astronomically driven, the tectonic process only set the boundary conditions necessary for the MSC to arise and glacio-eustatic sea level changes triggered the actual onset (Ohneiser et al., 2015). During the late Miocene, in the Messinian, there were periods of extended glaciation (Hodell et al., 2001; Lewis et al., 2008). An ice cap developed on Antarctica, but no major land ice formed on the Northern hemisphere. This meant that the climatic contrast between glacials and interglacias on the Northern was not as pronounced as it has been during the more recent glacial cycles of the Pliocene (Hodell & Kenett 1986). The driving factor of this Messinian glacial-interglacial cycle was obliquity with its period of 41kyr (Hodell et al. 2001).

3.2 Stages of the Messinian salinity crisis

A high resolution astronomical age model exists for the onset of the MSC. On Sicily, sediments of the MSC are directly underlain by cyclically bedded diatomites from the Tripoli Formation. These could be astronomically tuned to precession and give an age of 5.98 for the onset of the MSC (Hilgen & Krijgsman 1999). Studies in Greece, Spain and Cyprus found astronomic datings of 5.96 ± 0.02 Ma (Krijgsman et al., 1999; Krijgsman et al., 2002). The most complete succession was found in the Sorbas basin located in the south of Spain. This indicates that the onset of the Messinian salinity crisis occurred at 5.97 (Manzi et al. 2013). The onset was nearly synchronous across the Mediterranean, but to eliminate any local diachronous element for the age of the MSC, Manzi et al. (2013) proposed the use of the complete and sustained disappearance of micro planktonic assemblages as a marker for the onset of the MSC.

The most widely accepted interpretation of the MSC divides the crisis into three stages. Stage one (5.97-5.6 Ma) is marked by the onset of evaporite deposition in the Mediterranean. Stage two (5.6-5.53 Ma) has the acme of evaporite deposition in the deep basin settings. In stage three (5.53-5.33 Ma) the fossil assemblages show brackish water affinities and yet there are also signs of continued evaporite deposition. At 5.33 Ma the MSC was terminated by the Zanclean flood.

3.2.1 Stage one (5.97-5.6 Ma)

The onset of the MSC is marked by the deposition of thick layers of gypsum in the peripheral basins of the Mediterranean Sea. This indicates that evaporite precipitation and/or preservation was limited to the shallow water depths. De Lange & Krijgsman (2010) proposed a mechanism that allowed for basin wide gypsum precipitation, which was only preserved at shallow water depths during this stage. In the mechanism these authors hypothesize, saline water masses in a basin lead to density stratification and

the limited mixing of the water bodies prevented bottom water aeration, which can lead to anoxic bottom waters. Sulfate is an important oxidant for the degradation of organic matter in anoxic conditions (Chester, 2009). Because gypsum incorporates sulfate (Klein et al., 1993), it is only formed and preserved when sulfate is above the saturation point. The balance of sulfate supply versus organic matter degradation would then lead to a sulfate compensation depth, below which gypsum is not preserved (de Lange & Krijgsman, 2010).

The unit associated with the evaporites formed during stage one of the MSC is called the Primary Lower Gypsum Unit (PLG). The PLG has a rhythmic alternation between beds of massive brown selenite and thinner shale (Lugli et al., 2007). That alteration has been interpreted as a continuation of the precession controlled cyclicity of the underlying deposits (Hilgen et al. 2007). It has not been possible to verify this interpretation independently, but the ages that come with its use fit with other evidence (Roveri et al., 2014; De la Vara et al., 2015).

The alternation of selenite and shales indicates a climatic variation between dry and humid conditions at the frequency of precession. The African monsoon is commonly linked to precession. Northern hemisphere summer insolation maxima intensify the monsoon and cause more humid conditions, while the summer insolation minima are associated with weaker or absent monsoons and drier conditions (Gladstone et al., 2007). Thus the African Monsoon, would be the most obvious mechanism to carry the precession signal to the Mediterranean sediment and not the glacio-eustatic sea level changes which were controlled by obliquity.

In the marginal to intermediate basins, the top of stage one is an erosive surface, known as the Messinian erosional surface (MES). The MES shows signs of prolonged subaerial exposure, which indicates a sea level fall (Roveri et al., 2014). It has been dated at 5.61 Ma by assuming continued precession controlled cyclicity for the rhythmically alternating beds of the PLG.

3.2.2 Stage two (5.6 - 5.53 Ma)

This stage represents the acme of evaporite deposition, which was concentrated in the lower basins. The MES was formed during this stage and it is usually interpreted as a sign of a large sea-level drop, even though notions exist that it is a largely diachronous facies of a polygenic nature (Lofi et al., 2011).

The main deposit of the second stage is the Resedimented Lower Gypsum (RLG), which is marked by thick halite and clastic gypsum deposits. It lies on top of the MES and the clastic gypsum is interpreted as redeposited material from the basin's margin (Roveri et al., 2014). The erosion and mass wasting during the formation of the MES transported large volumes of gypsum to deep basins. It is likely that the rapidity of this process limited the time to dissolve gypsum as well as the degree of sulfate undersaturation in the bottom waters. Residementation of earlier precipitates could mean that the evaporite drawdown occurred over a longer period over the whole Mediterranean and that it was only transported to the deep basin setting in stage 2.

Halite has the largest volume of all potential evaporites that can be formed from the precipitation of sea water (Warren, 2010). This means that great volumes of evaporite would naturally precipitate at the highest rates when the hydrological balance of the Messinian Mediterranean Sea was at or beyond the concentration at which halite precipitates. If large parts of the Mediterranean became

exposed to these conditions during stage two this can explain the concentration of deposition in this interval.

Of all the evaporite formed during this stage the best studied facies are in the margins of the basin and in some sub-basins. The K-Mg salts deposited during this process show small scale lithological rhythmicity. These varves have been linked to annual and interannual cycles such as Quasi-Biennial Oscillation, El Niño Southern Oscillation, and decadal to secular lunar- and solar-induced cycles (Manzi et al. 2012). This means that even during stage two the halite precipitation was not continuous. It could even mean that the main part of the halite precipitation could have taken place during a few thousand years (Roveri et al., 2008; Manzi et al., 2012).

To generate the conditions for halite deposition during stage 2 there must have been little or no outflow from the Mediterranean to the Atlantic, while the volume of evaporite deposited means there must have been at least episodic inflow (Hilgen et al., 2007; Warren, 2010). In the relative sea level curve constructed by Ohneiser et al. (2015) the beginning of stage two at 5.6 Ma coincides with a lowstand due to maximal glaciation. This may have triggered beginning stage two, but the following deglaciation of TG9 did not terminate these conditions.

The basin wide tectonic activity across the Mediterranean that is associated with the second stage is a likely contributing factor to the conditions seen during stage 2 (Duggen et al., 2003). The high rate of deposition crust loading and the resulting isostatic rebalancing would have been a strong factor controlling the shape of the North Atlantic-Mediterranean gateway and thereby the hydrology of the Mediterranean (Govers et al. 2009).

The end of stage two has been approximated in two ways. First there is the downward tuning from the base of the Pliocene. The overlying deposits from stage 3 show a cyclicity that is presumed to be precession controlled (Manzi et al., 2009). The second method is a U-Pb zircon dating of an ash layer in the basal part of the post-evaporitic unit in the Apennines (Cosentino et al., 2013). Both give a similar end date of ca. 5.53 Ma.

3.2.3 Stage 3 (5.53 - 5.33Ma)

During the third stage, often referred to as Lago Mare, findings seem counterintuitive. Fossil assemblages indicate brackish conditions, but there was also continued evaporite deposition, which indicates elevated salinities (Roveri et al., 2014). The geochemistry of the bedrock around the Mediterranean is such that the freshwater influx from the local drainage area carries a distinct $^{87}SR/^{86}SR$ value that is lower than that of water from the Atlantic Ocean (Roveri et al. 2014). For stage 3, the $^{87}SR/^{86}SR$ ratio indicates a large fluvial influence (Roveri et al., 2014; Flecker et al., 2015). Fossils with Parathethian affinities and commonly associated with brackish to freshwater conditions have also been found in much of the Mediterranean. Together, these signs are indicative of a strong influence by the Paratethys on the Mediterranean and restrictions of the gateway between the Mediterranean and the Atlantic.

The Paratethys has many sills, these make its hydrological budget sensitive to shifts in local sea level changes (Krijgsman et al., 2010). If the Paratethys was a major source for the fresh water input of the Mediterranean, this sensitivity might explain the episodic evaporite formation in a largely hyposaline

environment. If the hydrological budget of the whole Lago Mare system was close to its hydrological equilibrium point, then this could explain how the basin hydrology changed so rapidly (Flecker et al., 2015; Gladstone et al., 2007). With the complete system close to equilibrium a relatively small shift in precipitation patterns could shift the entire system from a brackish water surplus to a shortfall with precipitation.

3.2.4 The Zanclean flood (5.33Ma)

The Zanclean flood event, marks end of the MSC. The Zanclean flood GSSP was defined by the base of the Turbi marls in Sicily and where the flood is dated at 5.33 Ma. This was done with cyclostratigraphy and isotope stratigraphy, the dating is well constrained with paleomagnetic data (Van Couvering et al., 2000).

The Zanclean flood caused the restoration of full marine conditions by opening the Gibraltar Strait and thereby ending the precipitation of evaporite in the Mediterranean Sea. The Zanclean flood was a geologically instantaneous event that was basin-wide and synchronous over that whole setting (Roveri et al., 2014). In some parts of the basin, it might have taken as much as three precession cycles before full marine circulation was restored (Iaccarino & Bosio, 1999). After the Zanclean flood and the opening of the Strait of Gibraltar the gateway between the North Atlantic Ocean and the Mediterranean Sea has been open. With the restoration of oceanic conditions, some of the deposited halite would have been eroded and mixed into the waters of the oceans.

Ohneiser et al., (2015) showed that the Zanclean flood coincides with a rapid deglaciation at TG5 ca. 5.33 Ma. Thus, relative sea level rise led to the reintroduction of full marine conditions, even though the even greater deglaciation at TG9 ca. 5.48 Ma did not cause a reopening. One explanation for the failure of TG9 to trigger reflooding is that the barrier at the North Atlantic gateway was more formidable at 5.48 Ma than it was at 5.33 Ma. Though it is possible that the barrier was degraded by a slow working mechanism and that the Zanclean flood is not directly related to a deglaciation. Water transport by seeping through faults that then led to failure of the barrier has been suggested as such a mechanism (Riding et al., 1998; 1999; Kamikuri et al., 2007). As with the rest of the MSC, the most likely explanation for the timing of the Zanclean flood is that local tectonic forces created the boundary conditions perhaps in combination with other forms of degradation of the barrier, which then allowed relative sea-level change to trigger the event, although much about the configuration of the North Atlantic-Mediterranean gateway during the MSC remains an open question.

3.3 Levantine deep basin model

In a recent publication based on data from the Levantine basin (one of the deep basins in the Mediterranean Sea) it has been found that the halite deposition in the deep basins started at the onset of the MSC and that no acme in precipitation was observed (Meilijson et al., 2017). A continuous sedimentary record was retrieved from a deep basin in the Eastern Mediterranean. By making an age model for this record, the timing of events in the deep basin setting could be studied directly. This record indicates that the onset of halite precipitation was synchronous with the beginning of the MSC in shallower settings and that precipitation was continuous over the whole MSC.

For their age model, Meilijson et al. (2017) used bio-events to date the pre-evaporitic shales. Based on these markers, the pre-evaporite deposition ceases and evaporite deposition begins at 5.94 Ma. Gamma-ray and resistivity well-logs that were made of the evaporite deposits and these logs reveal

a rhythmic component. In spectral analysis, 31 cycles in the 20 kyr frequency band were found. These cycles represent 620 kyr and thus cover the whole period of the MSC. The overlying interbedded evaporites were interpreted as deposits from stage three. This led to the conclusion that there was continuous deposition during the whole MSC, without any sign of an acme of deposition during stage two.

While this age model is theoretically coherent, there are no independent time constraints for the period of evaporite deposition. Spectral analysis can generate false positives when it is not integrated into a wider stratigraphic framework (Vaughan et al. 2011). A paleosalinity reconstruction of the North Atlantic Ocean could give some independent verification of the age model of this core. Continuous precipitation without an acme would lead to more gradual salinity decline than an abrupt deposition over just 50 kyr of the acme during stage two. Thus, the paleosalinity record of the North Atlantic Ocean could add to the interpretation of these findings.

3.4 Paleosalinity

The volume of salt deposited on the Mediterranean Sea-floor during the MSC is up to a million cubic kilometers (Roveri et al., 2014). In combination with the salt deposited in the area around the Red Sea in the early part of the Miocene, the draw down would have been 5% of the salt dissolved in the world's oceans (Ryan, 2009). The likely effect of such a draw down would have been a rapid decline of salinity in the open ocean (Berner & Berner, 1987). Salt deposition withdraws salt from the world's oceans until it is dissolved or eroded (Warren, 2010). Thereby deposition lowers the salinity of the open ocean until the deposits are mobilized and returned to the ocean. Thus, the salt drawdown during the MSC should have lowered the salinity of the world's oceans.

3.4.1 Paleosalinity proxy

Wit et al. (2013) proposed a proxy for salinity in the form of the Na/Ca ratio. With laser ablation mass spectrometry, the Na/Ca ratio in foraminiferal tests was measured. This measurement showed that Na is incorporated into the crystal lattice of calcite and that the concentration of Na^+ in the calcite test becomes greater at higher salinities. Wit et al. (2013) observed this in organic calcite and Okumura & Kitano (1985) showed the same result in inorganic calcite. These findings allowed Wit et al (2013) to determine salinity values based on Na/Ca ratios.

Besides salinity, both the growth rate and size of the tests correlate to Na/Ca ratio (Wit et al., 2013). These factors correlate to salinity as well, which could reinforce the salinity signal; however, in natural conditions, many other factors besides salinity could influence growth rate and size. Another possible concern is the chemical stability of the Na^+ in the calcite lattice, which may not be sufficient to preserve the Na/Ca ratio over millions of years (Evans et al. 2015). Post-depositional overgrowth of the calcite lattice is another factor of concern for paleoenvironmental use (personal communication E. Geerken, 2016). Despite the above-mentioned limitations, Na/Ca could still prove to be a suitable proxy for the purposes of this study.

4. Materials and Methods

4.1 Sample Material

The waters most immediately exposed the Mediterranean drawdown are the surface waters of the North Atlantic Ocean, as they are the source of the Mediterranean inflow water (Oddo et al., 2009). Thus, planktonic foraminifera from the North Atlantic will be studied. To eliminate any local terrigenous influence, an off-shore site in the North Atlantic is preferred, such as ODP site 982.

Hodell et al. (2001) developed an age model for the ODP core 982 which covers the whole duration of the MSC. The gamma ray attenuation bulk intensity (GRA) of the record was measured. Higher bulk density and carbonate content coincided with lower values of $\delta^{18}O$ in both the bulk carbonate and benthic foraminifers. This indicates that surface and deep waters were relatively warm. This was used as the reason for tuning the bulk GRA record to the precession dominated signal of the summer insolation at 65 °N. The coiling change of *Neogloboquadrina acostaensis*, which had been dated at 6.36 Ma in the Mediterranean (Hilgen & Krijgsman 1999), was used as the start for the tuning. The resulting age model is not unlike the result achieved by Baumann & Huber (1999) for ODP core 985. There the unfiltered carbonate record for the Plio-Pleistocene was linked to the summer insolation at 65 °N. The tuning of the bulk GRA record works particularly well for the interval from 6.4 Ma to 5.3 Ma because the GRA record carries a signal with a strong precession and obliquity component. In the pre-evaporitic Messinian this even allowed bed to bed correlation to the Mediterranean record in Sicily (Hilgen et al. 2007). This optimal interval for the tuning covers with the whole MSC. These factors together mean ODP 982 is well suited to the purposes of this study.

The ODP 982 core was visited in the ODP core repository in Bremen University and sampled at a 10-cm interval. To capture the period with the greatest possible salinity offset within a limited set of samples, two intervals were chosen: an older section covering much of stage two and the onset of stage 3 and a younger interval just before the Zanclean flood. The older sampled interval covers the range from MCD 174.12 to 169.66 of the splice of ODP core 982 (Jansen et al., 1996). The samples for this interval were taken from the between TG 9 and 14, covering a 140 kyr period between 5.582 Ma and 5.554 Ma. The younger interval covers the shorter interval from 165.24 to 163.84 of the splice of ODP core 982. In the age model this covers an interval from 5.369 Ma to 5.336 Ma. These ages are based on the age model as described by Hodell et al. (2001).

To reconstruct a salinity from the Na/Ca ratio a calibration curve is required. Therefore specimens of the selected species of foraminifera that lived at a known salinity are necessary. The samples from the cruise 64PE275 were used to acquire such specimens. The salinity measurements made during the cruise were used to determine a salinity at each sampling location. Since the area covered in the cruise is close to the Rockall Plateau, this was the closest approximation possible for the foraminiferal assemblage of the samples covering the MSC in the ODP 982 core.

To establish the calibration curve, five samples were chosen to give an even spread across the maximal range of salinity. The salinity ranged from 34.5 practical salinity unit (psu) to 35.5 psu. This range is relatively narrow compared to the nine psu used in Wit et al. (2013), but in the natural conditions of the open ocean, in a region where the picked species live and are deposited, this is the greatest naturally occurring range (personal communication G. J. Brummer).

4.2 Sample Preparation

The samples from the ODP 982 core were treated per the standard ODP sample preparation model. Both the material from ODP 982 core and 64PE275 was wet sieved. With three stacked sieves the material was separated into three size fractions; >150 μm, > 63μm, and >38μm, respectively. Some of the samples from the 64PE275 transect contained very coarse material, for these a fourth sieve of > 0.5cm was used at the top of the stack. Later, it turned out that the foraminiferal content of these samples with very coarse material was so low that the samples were not suitable for picking and, thus, these sample were not used in the rest of the study. After the sieving the samples were dried for 24 hr. in an oven at 40°C. The samples from the >150 μm fraction were all halved with a splitter. This was done so that one half could be put in storage; the other was used in the rest of the study.

4.3 Selected foraminifera

As previously explained in a planktonic foraminiferal species was the best suited to the purposes of this study. *Neogloboquadrina acostaensis* was selected as the main species in the ODP 982 record because of its continuous presence in the record of ODP core 982 (personal communication M. Tulbure 2015; Jansen et al., 1996). For the shorter younger interval *Neogloboquadrina atlantica* was also collected.

For the calibration curve, the species also had to be present in the samples from the transect of the 64PE275. The *Neogloboquadrinid* species found in the ODP 982 core are extinct which required the selection of an analog. Morphologically the specimens of the modern *Neogloboquadrina incompta* in the core material from the 64PE275 transect were closest to *N. acostaensis* as found in ODP 982, both in size and in form.

Aze et al. (2011) constructed a phylogenetic tree of Neogloboquadrinids (Figure 2). This tree can be used to gain insight into the relations between the Neogloboquadrinids. The research into the evolution and phylogeny of Neogloboquadrina is limited and leaves holes in our knowledge of the species. This phylogeny is based on morphological data and it does not include all known forms of Neogloboquadrina. For this study, the main limitation is the complete absence of *N. atlantica* from the tree. Since the distinction between *N. incompta* and *Neogloboquadrina pachyderma* is based on genetic insights, they have not incorporated it either. Still, it is the most complete phylogenetic tree available and it does show the relation between *N. acostaensis* and *N. incompta*.

Figure 2. *The phylogenic tree of Neogloboquadrina from Aze et al., 2011*

4.3.1 Neogloboquadrina acostaensis

N. acostaensis are an extinct morphospecies, with its first occurrence at 10.55 Ma (Hilgen et al., 2000). The species is found in Mediterranean as well as Atlantic samples. The species is thought to have evolved in the North Atlantic Ocean. It seems likely that the *N. atlantica* was ancestral to the *N. acostaensis* (Zachariasse, 1992). The most current evidence suggests that the *Neogloboquadrina dutertei* evolved from *N. acostaensis* in the Miocene (Ujiié & Ishitani, 2016; Aze et al., 2011).

The following species concept was applied here; *N. acostaensis* has 4 to 4.5 chambers in the final whorl (Figure 3). The selected specimens have a wall with a honey comb structured or cancellate wall, though various stages of wall thickening could be found. Kummerforms and apertural lips were common, but specimens with these features were avoided during the picking process. Adult forms of this type are close in form to juvenile *N. atlantica*, but they can be distinguished because their back coil is flatter and the main coiling direction was sinistral for the *N. acostaensis* and dextral for the *N. atlantica*. The umbilical position of the aperture that can occur in *N. atlantica* is another distinguishing feature.

4.3.2 Neogloboquadrina atlantica

N. atlantica represents a discrete late Miocene to late Pliocene species indigenous to the mid to high-latitude North Atlantic (Berggren, 1972). Its size and shape show a high degree of variability (Poore and Berggren, 1975). This included intergrading of small forms of *N. atlantica* with *N. pachyderma*, possibly including juvenile forms. There were several episodes where *N. atlantica* invaded the Mediterranean Sea (Zachariasse et al., 1990). The species is thought to have gone extinct in the North Atlantic at 2.4 Ma (Weaver & Clement, 1986).

N. atlantica is a 4 to 5 chambered globigerinid with a cancellate wall (Figure 3). In its adult form the *N. atlantica* is considerably larger and has thicker walled tests than the *N. acostaensis* and can also be recognized by the umbilical position of the aperture. In the assemblages from the MSC interval at site 982 it is mainly dextrally coiled, as is common for Messinian deposits.

4.3.3 Neogloboquadrina incompta

N. incompta is mainly found in the Northern reaches of the Atlantic Ocean. Since it is currently extant, the molecular heritage of the taxon has been studied. Darling et al. (2006) found evidence that there is a genetic distinction related to the coiling direction in *Neogloboquadrina pachyderma*. It was proposed to refer to the mainly northern, dominantly sinistrally coiling group as *N. pachyderma*, while the dominantly dextral group associated with lower latitudes would be called *N. incompta*. There are specimens of the *N. pachyderma* genotype that show a dextral coiling direction and the opposite is true for *N. incompta*. These specimens are rare at 1-3% of the total population. In their study of morphological variation in *N. pachyderma*, Eynaud et al. (2009) indicated that there might be up to five distinct morphospecies within the group of dominantly sinistrally coiled *N. pachyderma* found in the North Atlantic Ocean. Darling & Wade [2008] find seven distinct groups based on their genetic analysis. There is no data to indicate how the five morphospecies correlate to the seven genotypes.

In the studied assemblages, *N. incompta* had a dextral coiling direction and was very close in form to *N. acostaensis*, with a cancellate wall and 4 chambers in the final whorl. Its coil is a little tighter than in the *N. acostaensis*. Since *N. acostaensis* is absent in assemblages after its extinction, the distinction is easy to make.
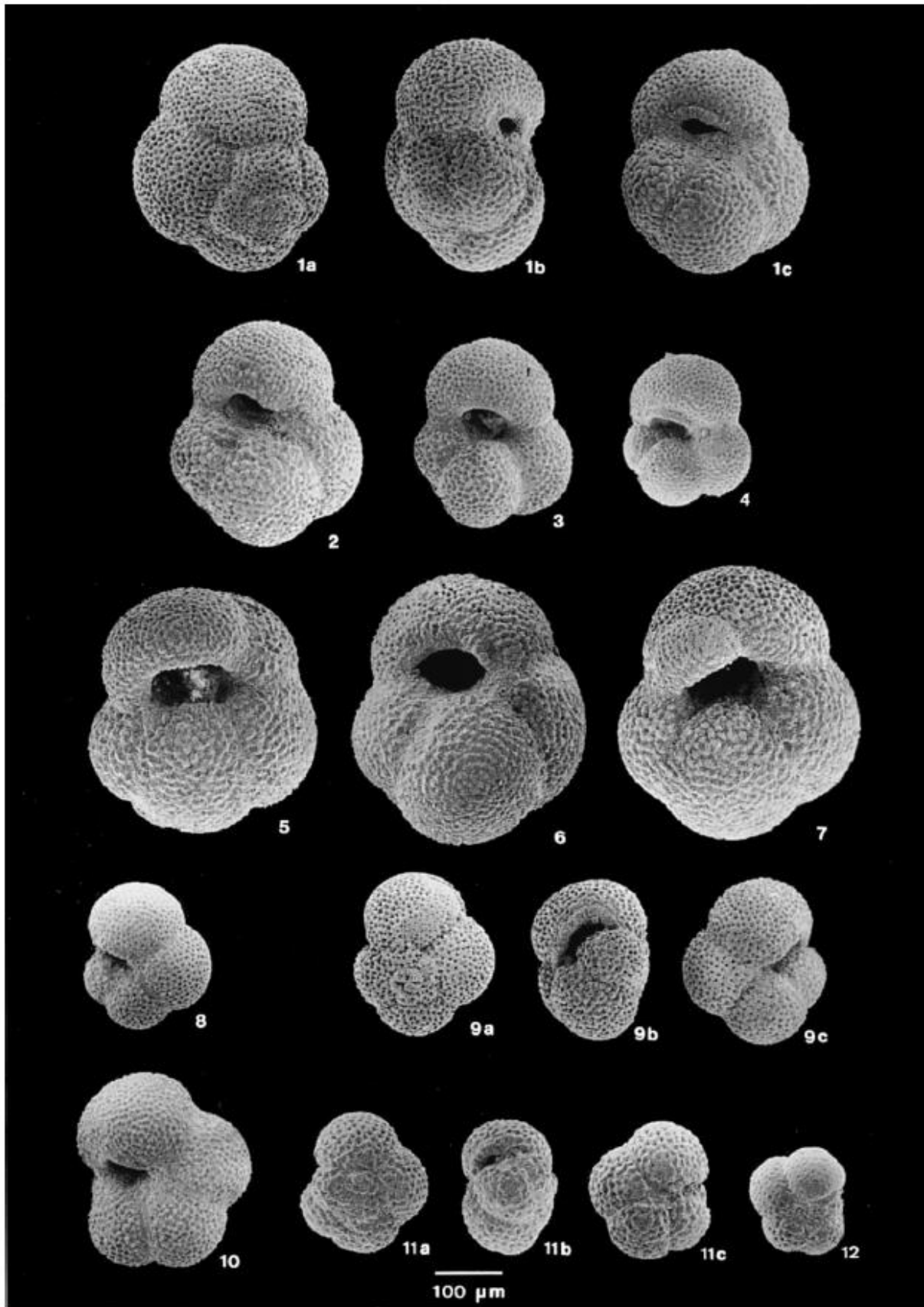
Figure 3. *Plate from Hilgen et al. (2000) 1-4 Neogloboquadrina Atlantica (small sized); 5-7 Neogloboquadrina Atlantica large sized. 8, 9, Neogloboquadrina 4-chambered type. 10 – 12 Neogloboquadrina acostaensis*

4.4 Picking process

The foraminiferal specimens were picked with the use of an optical microscope. To speed up the picking process both supervisors of this thesis, as well as the writer, picked specimens from the samples. To keep the process consistent, the second supervisor (M. Tulbure) made a final inspection of all the picked specimens. The minimum mass of material required for the analysis was 400 µg, the total weight of the picked specimens was determined. The number of weighed specimens was then counted, so that the mean weight per specimen could be calculated. More were picked if the mass of the collected specimens was below 400 µg.

To minimize the variance within each sample only sinistrally coiling *N. acostaensis* were picked. In two samples, dated at 5.580 and 5.583 Ma, the occurrence of sinistral *N. acostaensis* was so low that it proved to be impossible to reach the minimum mass for analysis with sinistral specimens. We chose to replace the sinistral *N. acostaensis* with dextrally coiled *N. acostaensis*. These two data points are clearly labeled to indicate this in all graphs where they are included.

In the younger section from 5.369 Ma to 5.336 Ma, the specimens were collected in threefold to illuminate the species effect: specimens were collected once for each of the coiling directions of *N. acostaensis* and once for *N. atlantica* dextrally coiled. Since the conditions in the open ocean were similar for all three populations, they could give insight into the reliability of the Na/Ca record as well.

4.5 The cleaning process and analysis

A version of the Cambridge protocol based on Barker et al. (2003) modified at the Royal Netherlands Institute of Sea Research (NIOZ) was used to prepare the sample material for measurement. The samples were cleaned in a clean room. Various steps were taken to remove coccoliths, clay, and organic matter. At this point a fraction of the sample matter was split off for the stable isotope measurement and the rest was used for the ICP-MS measurement. The cleaning protocol to prepare the samples for dissolution ICP-MS is described in detail in the appendix A.

To use the ion coupled pulse mass spectrometer (ICP-MS) works so each sample was dissolved. To achieve maximum accuracy the Element-2-ICP-MS requires a concentration of 20 ppm Ca. Thus, all sample concentrations were determined with by ICP-MS. These concentrations were then used to dilute the remaining 240µl of all the samples to a concentration 20 ppm Ca. All diluted samples were run through the Element-2-ICP-MS to determine the composition. The diluted volume of some of the samples was large enough to allow for more than measurement of the same sample. With these extra measurements, the precision of the measurement could be tested. To test accuracy during the ICP-MS measurement various lab standards were included in each run, with these any detected drift was corrected.

The material for the stable isotope analysis was separated from the rest of the material during cleaning process. The sample fractions were weighed at this point to give an indication of the amount of Ca in the test run. The samples were then run through a Gas GC/IRMS to measure the $\delta^{18}O$ and $\delta^{13}C$. In a Kiel IV Carbonate Device, the sample material was dissolved by dripping H_3PO_4 onto the material. The resulting gas was then fed to a Delta-Plus XP mass spectrometer. Various lab standards were used in the measurements to determine measurement accuracy. Any detected drift was then corrected. When the

accuracy was too low, the data from the run were discarded. Due to problems with the device, some samples were lost entirely or failed to deliver useable data. This was a mainly an issue for the samples from the younger Interval covering the period from 5.369 Ma to 5.336 Ma.

4.6 Corrections to the Na/Ca record

Na/Ca correlates to growth and specimen size (Wit et al. 2013). These factors vary from specimen to specimen per the conditions under which they developed. To control these factors and other sources of inter specimen variability as much as possible, a minimum of fifty specimens per sample was used. The number of specimens was counted for each sample, thus specimen size can be approached with the mean specimen weight per sample. The Na/Ca was plotted against mean specimen size per all the species measured and the correlation was calculated (Figure 4). The R^2 of the correlating line gives an indication of the strength with which the mean specimen size influences Na/Ca. As it was very low, no correction for mean specimen size was made.
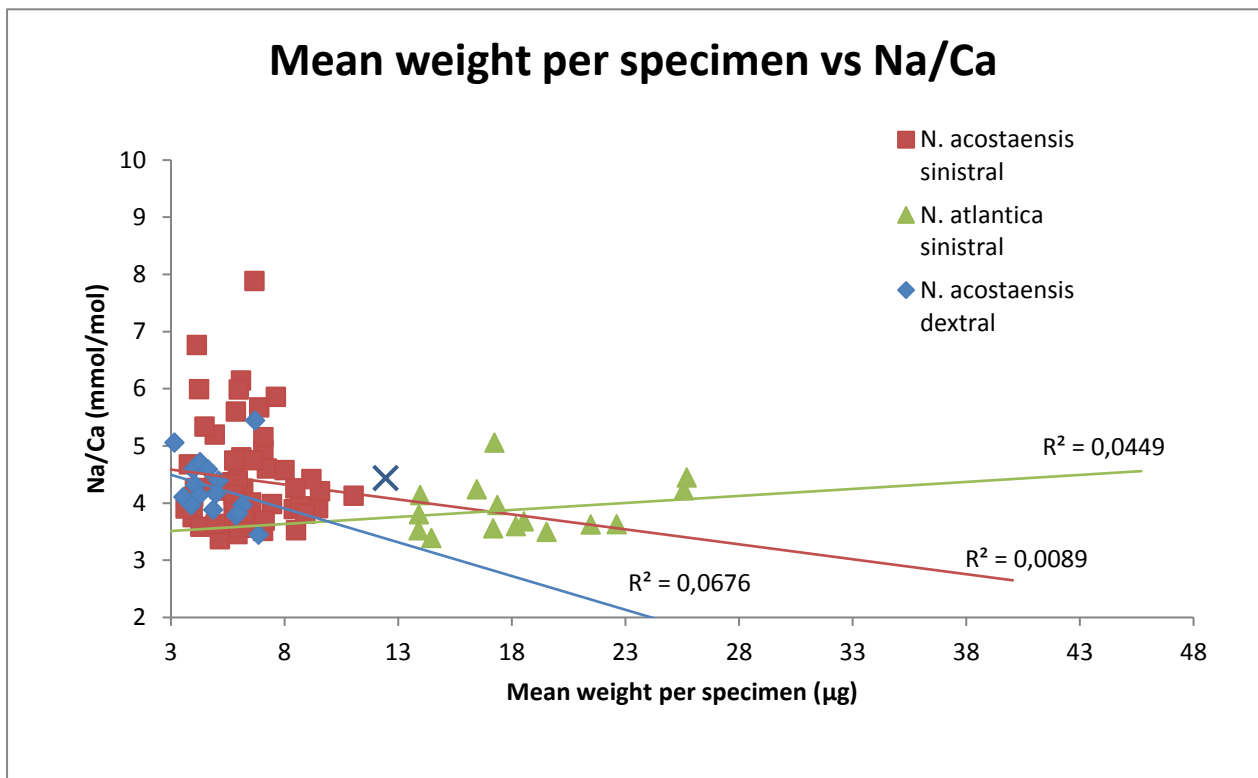

Figure 4. *The mean weight per specimen versus the Na/Ca ratio. The blue cross represents an aberrant measurement for dextral N. acostaensis, which was not used to calculate the trend line. The trend lines for each population are shown in their respective colors with their R^2 values.*

Because dextral *N. acostaensis* were used in two samples, it should be checked if there was a detectable difference in the rate at which Na/Ca is incorporated into the calcite lattice of the tests of sinistral and dextral *N. acostaensis*. The Pearson correlation index between the two species was calculated to evaluate the strength of the correlation (see Table 1). This correlation was 0.49 indicating

that 51% of the variation in dextral Na/Ca was not explained by variation in the Na/Ca of the sinistral species. This was still judged to be strong enough to proceed with a correction for the species effect. The correlation between Na/Ca in both species was calculated (equation 1, Figure 5). With this correction, the mean deviation in Na/Ca between the sinistral and dextral species was reduced from -0.63 to -1.65*10^{-4}, though the R^2 of the fit is only 0.24. The same correction was applied to the two dextral samples of *N. acostaensis* in the older measured interval.

Eq 1.

$$Na/_{Ca}\,sinistral = 0{,}3959 * Na/_{Ca}\,dextral + 2{,}3404$$

Table 1. *The Pearson product-moment correlation coefficient was calculated to quantify the dependence between the two variables. The one measurement of dextral N. acostaensis that was found to be unreliable was not used in the calculation of the correlation.*

	For Na/Ca	For Mg/Ca
Sinistral and dextral *N. acostaensis*	0,491341	0,800986
Sinistral *N. acostaensis* with *N. atlantica*	-0,01095	0,404727
Dextral *N. acostaensis* with *N. atlantica*	0,00641	0,462469

Relation between sinistral and dextral *N. acostaensis*
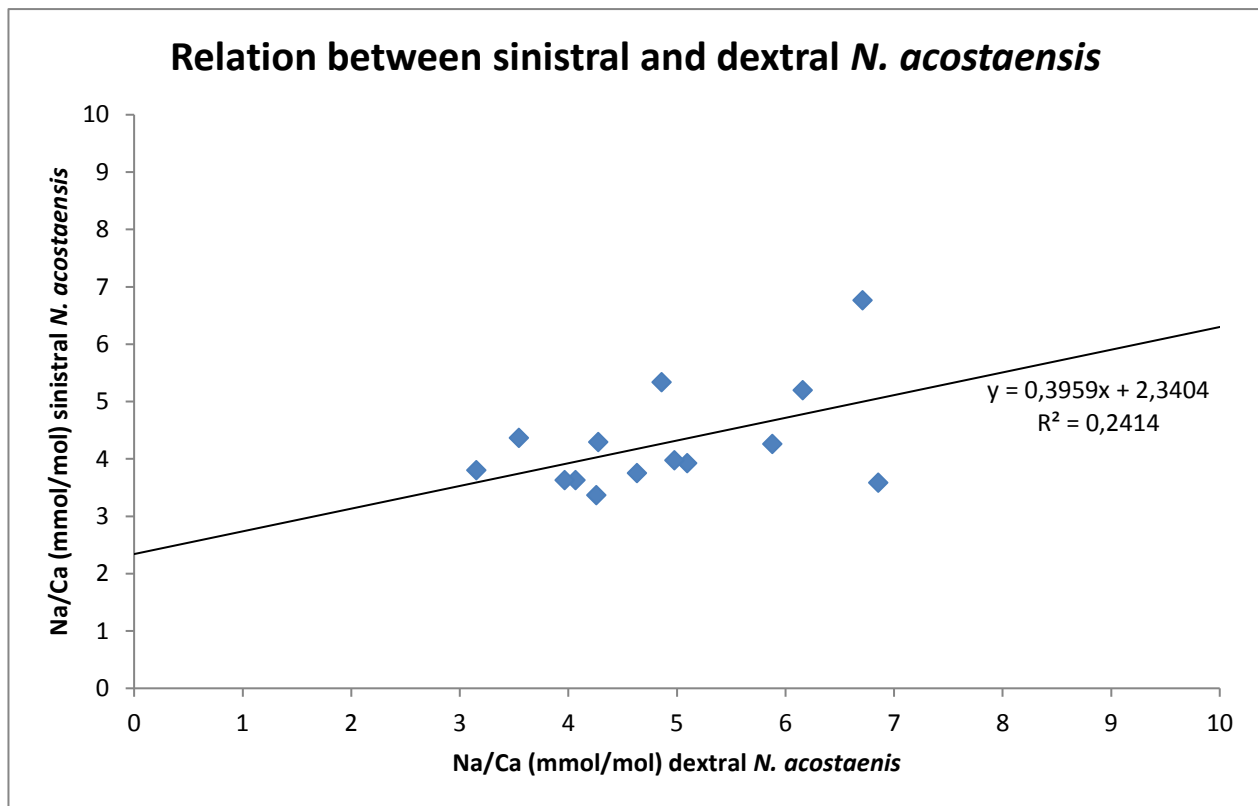
y = 0,3959x + 2,3404
R² = 0,2414

Figure 5. *A plot of sinistral and dextral N. acostaensis. A linear line was fitted through the data series to find a species effect.*

The Na/Ca measurements have great variability, to reduce this effect and increase legibility of the data a three-point moving average was used to calculate (see Figure 5). There were two outliers with Na/Ca values that were an order of magnitude outside of the range of the other measurements, these same samples also had aberrant results in their Mg/Ca values, indicating some error in the ICP-MS measurement. These two outliers were excluded from the smoothed data series.

The standard error of the measurement was calculated for samples that had been measured more than once. A ninety-five percent confidence interval was calculated by subtracting and adding twice the standard error to the data points. This was done to the data points of the three-point moving average series. For points where there was only one measurement, the 95% confidence interval was estimated by linear interpolation between the two nearest points where the standard error could be calculated. In the younger interval, no double measurements were available at all. The mean standard error of the whole lower series was used to estimate the standard error for this interval.
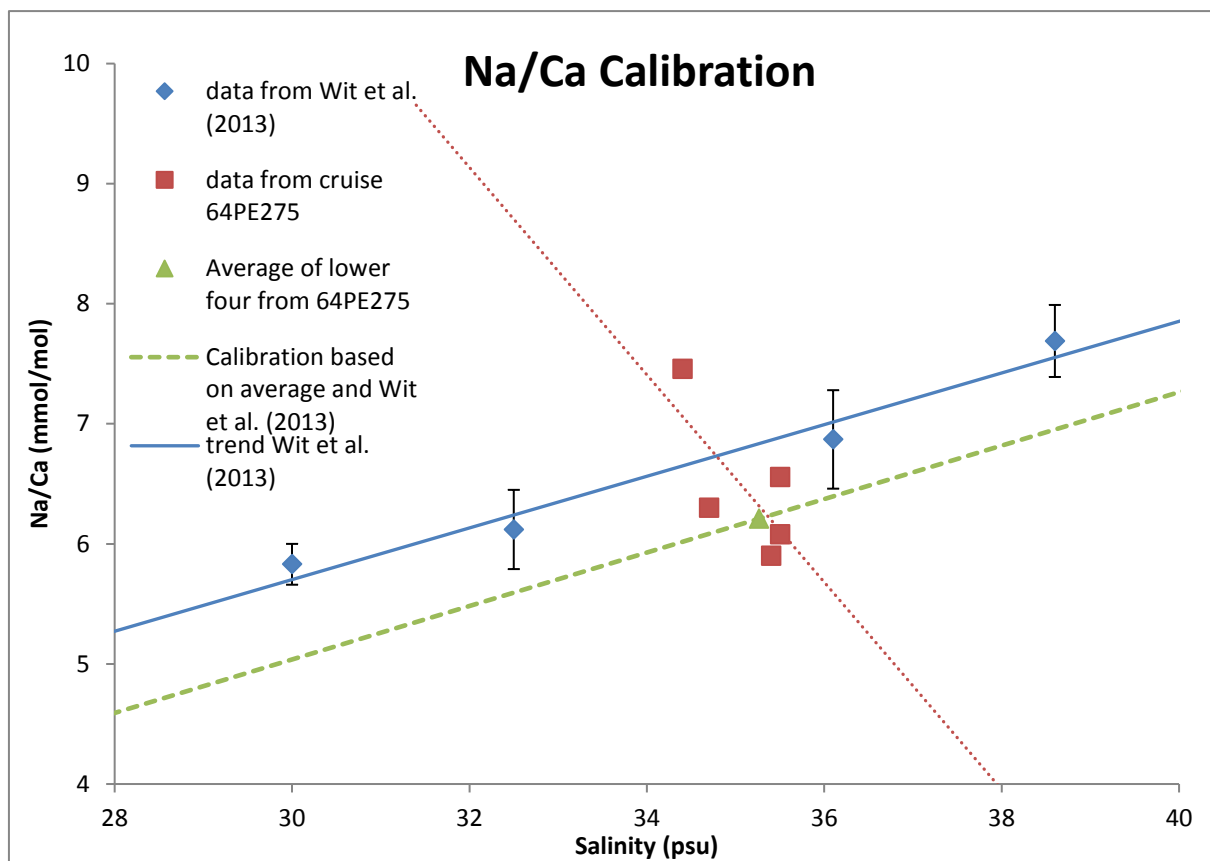

Figure 6. *The blue data points and trendline are based on the data from Wit et al. (2013). The red data points and trendline are based on measurements on samples collected from the 64PE275 cruise. The green data point is the average of the lower four measurements from the 64PE275 cruise. The green calibration line goes through the green data point and has the directional coefficient of the data from Wit et al (2013).*

4.7 Salinity calibration and Paleosalinity reconstruction

To link the Na/Ca values to salinity values, a calibration curve was made (Figure 6). The data from the 64PE275 cruise were used to determine the correlation between Na/Ca and salinity in *N. incompta*. This analysis indicated that the rate of Na incorporation decreased as salinity increased. Because this response goes in the opposite direction than all the published literature another method was applied

(Wit et al., 2013; Okumura & Kitano, 1985). The average Na/Ca from four clustered samples from the 64PE275 was used to set a point. Then a line with the directional coefficient of the correlation published by Wit et al. (2013) for *Ammonia tepida* was laid through this point. The calibration line generated in this way was then used to link Na/Ca in *N. acostaensis* to salinity values.

4.8 Estimating the salinity response

Both hypotheses of this study involve a shift in the paleosalinity. To test these a profile of the expected salinity profile was modeled. This requires two things: an estimate of the decline in salinity and an estimate of the natural ion fluxes that could compensate for the salt draw down in the long term. Ryan (2009) found that the volume of salt deposited in the Mediterranean and Red Sea area during the MSC was ca. 5% of the total amount of salt dissolved in the world's ocean at present. The salinity fall associated with this salt drawdown can be estimated by using the equation below:

Eq.2

$$salinity\ (psu) = \frac{salt\ (g)}{sea\ water\ (kg)}$$

Hence, a 5% decline in salinity would can be written as:

Eq. 3

$$\frac{0.95\ \% * salt\ (g)}{sea\ water\ (kg)} = 0.95\ \% * \frac{salt\ (g)}{sea\ water\ (kg)} = 0.95\% * salinity\ (psu)$$

The relative shifts in salinity are thus linearly correlated to a relative drawdown of salt from the world's oceans. The residence time of water in the oceans is ca 3-3.5 kyr (Marshak, 2011). Therefore, the salinity of the world's oceans would be expected to lag the drawdown by no more than 3.5 kyr.

The natural ion flux must also be estimated to create an expected salinity profile. One million cubic kilometers is a rough estimate of halite deposited in the Mediterranean over the duration of the MSC (Rover et al. 2014). The density of halite is 2.16 g*cm^{-3} (Hay et al. 2006). Together the data allows an estimation of the extent of the salt drawdown from the world's oceans in moles as given by eq 2.

Eq.4

$$mass\ of\ deposited\ halite = density\ of\ halite * volume\ of\ halite = 1.1 * 10^6 km^3 * 2.16$$
$$= 2.376 * 10^{15} kg$$

The current sodium chloride flux into the world's oceans has been estimated at $6*10^{11}$ mol yr by Chester & Jickells 2012. Hay at al. (2006) estimate the yearly flux to be between 1.1*10^11 kg*yr^{-1} and 4.21*10^11 kg*yr^{-1}. Given these fluxes equation 5 has been used to calculate the data in **Error! Reference source not found.**.

Eq. 5

$$time\ to\ replace\ the\ deposit\ down\ (yr) = \frac{mass\ of\ deposited\ halite}{yearly\ sodium\ NaCl\ flux\ (kg * yr^-)}$$

Table 2. The replacement time of the salt drawn down during the MSC, based on three estimates of the salt flux.

	Chester & Jickells (2012)	Min. flux Hay at al. (2006)	Max. flux Hay at al. (2006)
Flux (kg yr-1)	3.51*10^10	1.1*10^11	4.21*10^11
Time to replace (Ma)	67.8	21.5	5.64

The variance in the estimated replacement time is great, but even with the highest flux the replacement time still far exceeds the duration of the studied interval at 5.64 Ma. This would indicate that the major source of salinity over the studied interval is the deposition and erosion of salts, not natural fluxes.

The Zanclean flood and restoration of marine conditions on the Mediterranean Sea would have led to the erosion of halite. The volume of halite dissolved after the Zanclean is difficult to estimate (Hay et al. 2006). To give some indication of the expected results, 10% of the deposited salt volume is assumed to have been eroded due the Zanclean flood. Iaccarino & Bosio (1999) estimated that it took up 60 kyr before full marine conditions were restored in the Mediterranean after the Zanclean flood. It will be assumed that all salt that was dissolved due to the Zanclean flood, dissolved this 60 kyr period.
To create a shift in the salinity decline, it was assumed that half of all the halite deposited over the MSC was deposited in stage 2 and that the other half was deposited at the same constant rate in stage 1 and 3. Because of poor time constraints on the deep basin settings the rate of deposition is not known. The choice for these shifts in the rate of deposition was made because it would give a large contrast between the stages.

4.9 Evaluating reliability
The $\delta^{18}O$, $\delta^{13}C$, and the Mg/Ca were measured (Figure 7. A, B, and C respectively). These records can be used to check the reliability of the data. The variability of Na/Ca is greater than that of any of the other three measured series, this may be a sign that there is more random noise in the Na/Ca record. Possibly an indication of poor preservation. Neither $\delta^{18}O$ nor Mg/Ca show a pulse around the onset of stage three of the MSC, even though both proxies react to salinity (Ferguson et al., 2008). This does not confirm the observation of a salinity peak in the Na/Ca record. There is a $\delta^{18}O$ peak right at the beginning of stage three, but it does not have the same duration as the 43 kyr pulse seen in the Na/Ca.

In the younger measured interval, specimens in tri-fold and the relations of these three measurements can be studied. The Pearson correlation index between this data was also calculated (Table 1), it shows that the Na/Ca does not have a high correlation between both species of *N. acostaensis*, and the correlation between either of the *N. acostaensis* species and the Na/Ca in *N. atlantica* was very low. This indicates that the Na/Ca is influenced by many factors that act independently on the three species. Figure 8 illustrates the same point. For Mg/Ca the correlation is much higher and more easily observed. Together this data indicates that the preservation of Na^{+} was

probably poor and that post depositional processes may have acted differently on the larger tests of *N. atlantica*.

For δ^{18}O two benthic records covering the studied interval were compared to the *N. acostaensis* record retrieved from ODP core 982 (Figure 9). The relations between the benthic δ^{18}O and the planktonic record are not clear. In the younger interval at the end of stage three, the signals appear to be similar with an offset. The difference between the benthic and planktonic environment could explain that offset. The timing of events is similar enough that the records seem to overlap, but there are also big differences at the base of the record, around 5.55 Ma, there is a big peak in the benthic record of ODP 982, which cannot be correlated to any such event in the planktonic record. That the offset between the records is not constant shows that the difference between benthic and planktonic conditions varied over studied interval.
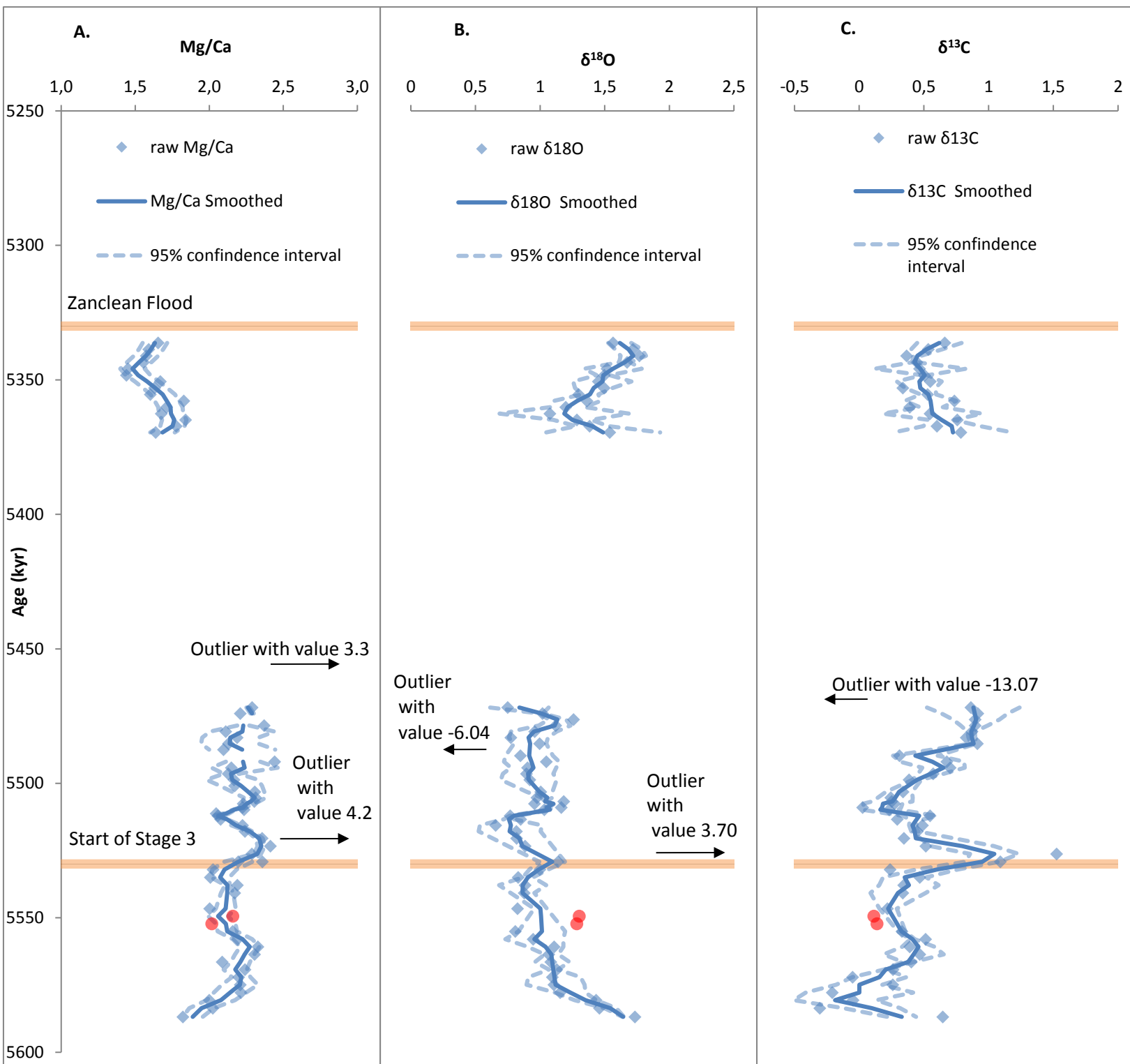
Figure 7. *The Mg/Ca; δ¹⁸O; δ¹³O from N. acostaensis from ODP core 982. The red circles represent two data points where dextral N. acostaensis were picked because sinistral specimens were nearly absent. Outliers that fall outside of the chart area are represented with a black arrow. These outliers were excluded from further calculation. The orange horizontal lines indicate the start of stage 3 of the MSC and the Zanclean flood. The data were smoothed with a three point moving average.*

    A.   *The Mg/Ca for N. acostaensis from ODP core 982. The two dextral samples were included in the moving average and the calculation of the confidence envelope.*

    B.   *The δ¹⁸O for N. acostaensis from ODP core 982. Here the two dextral samples were not included in moving average or the calculation of the error envelope.*

    C.   *The δ¹³C N. acostaensis from ODP core 982. Here the two dextral samples were not included in moving average or the calculation of the error envelope.*
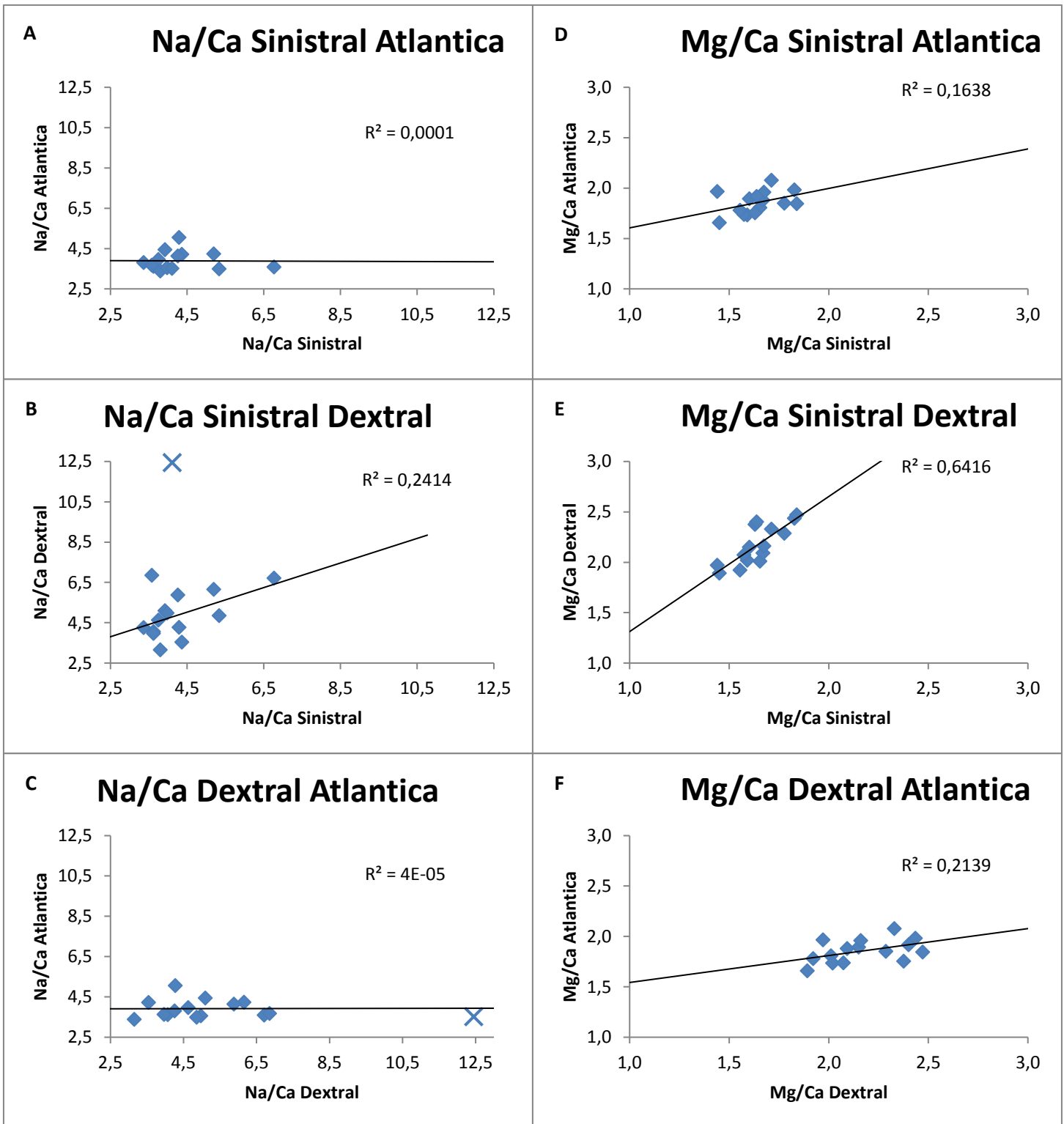
Figure 8. Showing the correlation between Na/Ca and Mg/Ca ratios for N. acostaensis sinistral, dextral, and N. atlantica, the black line is a best fit linear to the data. The R² for each fit is shown in the top right corner of the graph. One measurement of the Na/Ca ratio in dextral N. acostaensis is aberrant and was not used to generate the linear fit, it is represented by with a blue cross. It was not used to generate the trend line.
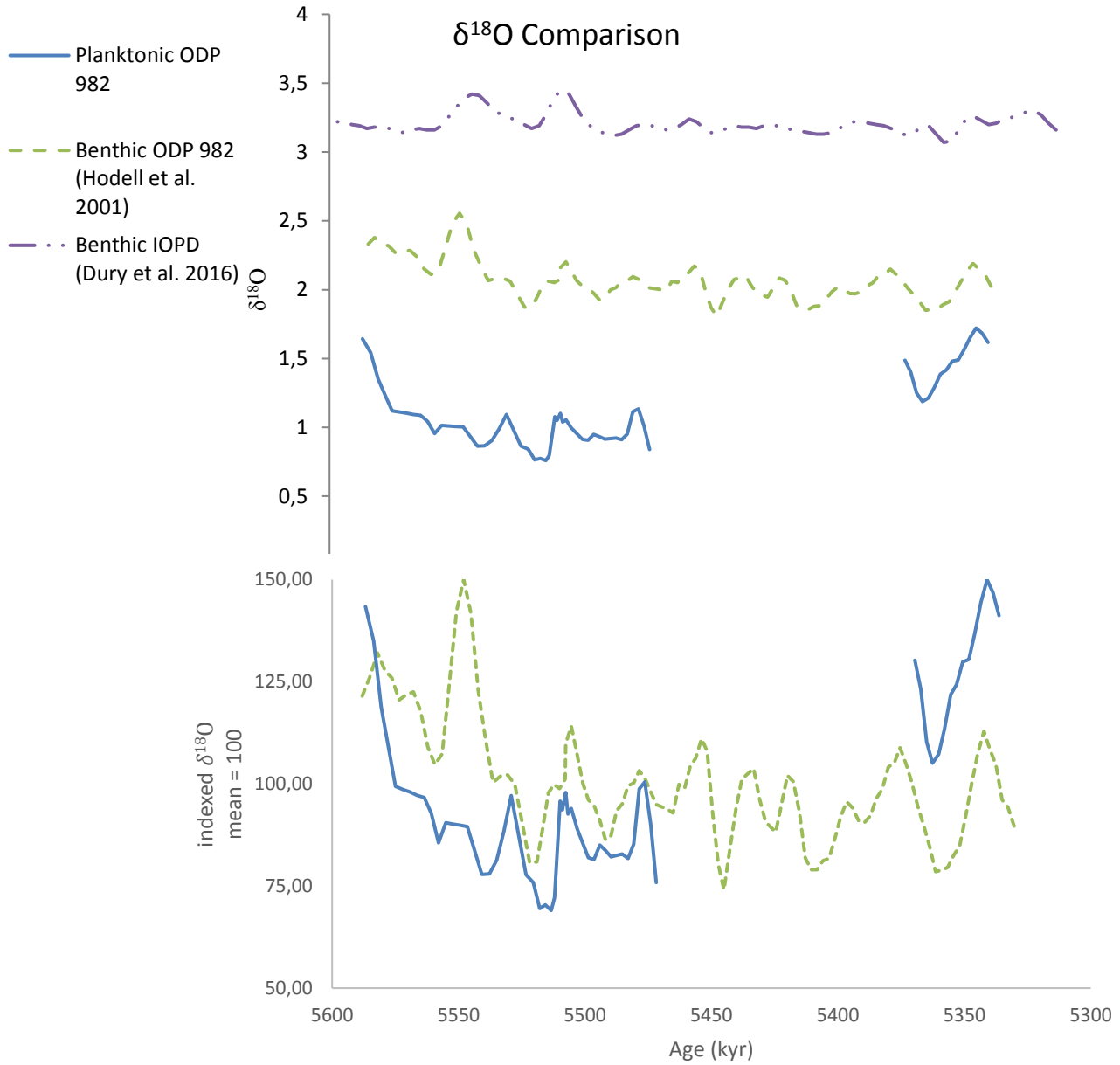
Figure 9. *Above the benthic and planktonic $\delta^{18}O$ records of ODP core 982 and the Benthic record of IODP 1338. Below to ease comparison between the benthic and planktonic records of ODP 982 these two were indexed to their mean. ODP site 982 is in the North Atlantic, IODP site 1338 is in the Southern Pacific Ocean.*

5. Results

The paleosalinity reconstruction can be broken down into two parts. The first part is a relative salinity profile, based on the assumption that there is some unknown but linear correlation between salinity and Na/Ca. The second part is a calibrated paleosalinity profile with absolute values for the salinity. The modeled salinity profile over the MSC can be compared to both profiles, to evaluate the data that is revealed (Figure 10).

The raw Na/Ca data is greatly variable and does not show any clear trend (Figure 11). This may be an indication that the data themselves were unreliable, or that some further processing was required. Thus it was attempted reduce the noise content of the Na/Ca record.

Figure 12 demonstrates an indication of the relative salinity change. It is assumed that higher Na/Ca relates to higher salinities, with a three-point moving average to smooth the data. The variability from point in the Na/Ca record remained after smoothing and the elimination of outliers. The 95% confidence interval shows the variation is not due to inaccuracy of the measurements, but it is inherent to the Na/Ca values of the samples. There is a variation around the mean value of 4.3 at the start and end of the measured interval. In between, at the beginning of stage three, there is a 43kyr pulse with high Na/Ca. Beyond this pulse, it is not clear if there is anything other than pure noise in the record. Thus, any conclusions about paleosalinity are tenuous at best.

To determine the absolute values of the salinity shifts, a calibration curve was made (Figure 6). The data from the 64PE275 cruise was used to make a trend line, which showed a decline in Na/Ca with increasing salinity. This was thought to be unreliable, because all other observations of the relationship between Na/Ca and salinity are in the opposite direction. A second calibration was made based on the data from the 64PE275 cruise and the data from Wit et al. (2013). With this calibration and the smoothed Na/Ca curve from Figure 12, the paleosalinity reconstruction shown in Figure 13 was calculated. This reconstruction showed a highly variable salinity profile that is oddly stable over the long term. Over the whole measured interval, the salinity varies between a minimum of 25 psu and a maximum of 35 psu, but the average of the fifteen youngest data points is almost the same as the average of the fifteen oldest data points. This means that no net drawdown of salt was detected over the course of stage 2 and 3 of the MSC. In between at the onset of stage 3 there is a 45 kyr pulse of high Na/Ca values, which goes up for 25kyr, then falls back down to some of the lowest values in the record in 18 kyr.

These results do not show a direct link between the salt drawdown in the Mediterranean basin and paleosalinity in the North Atlantic, as based on Na/Ca as a proxy for paleosalinity. The timing and magnitude of the Na/Ca pulse at the onset of stage 3 are intriguing, but without further corroboration the Na/Ca record made in this study does not seem reliable enough to support any further conclusions on its own.
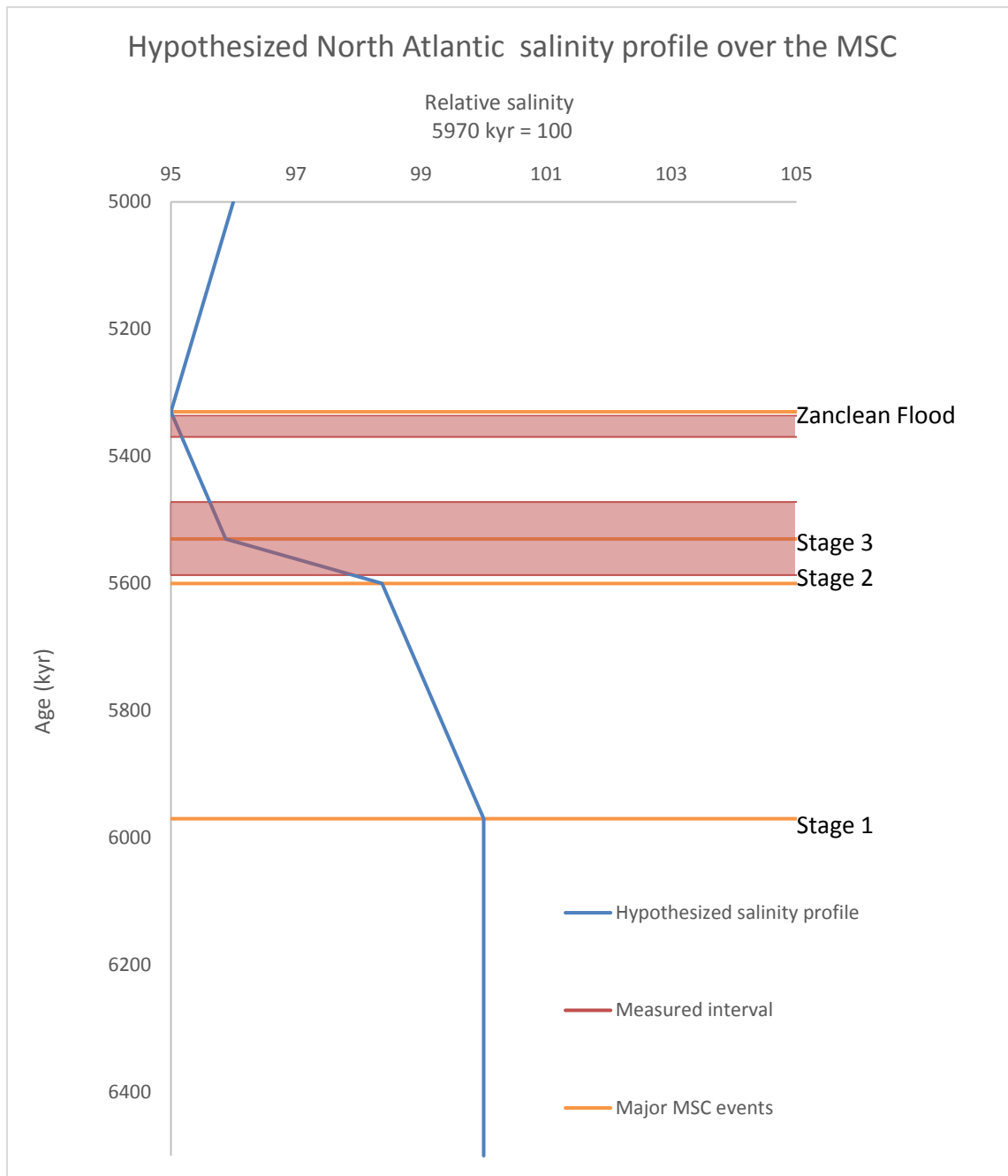
Figure 10. *The hypothesized North Atlantic salinity profile. The measured intervals are colored in red, the orange lines indicate the major events of the MSC. The hypothesized salinity profile shows a drawdown in during the whole MSC, with the most rapid deposition in stage 2. After the Zanclean flood part of the deposited evaporite is dissolved and brought back into the ocean, this increases the salinity.*
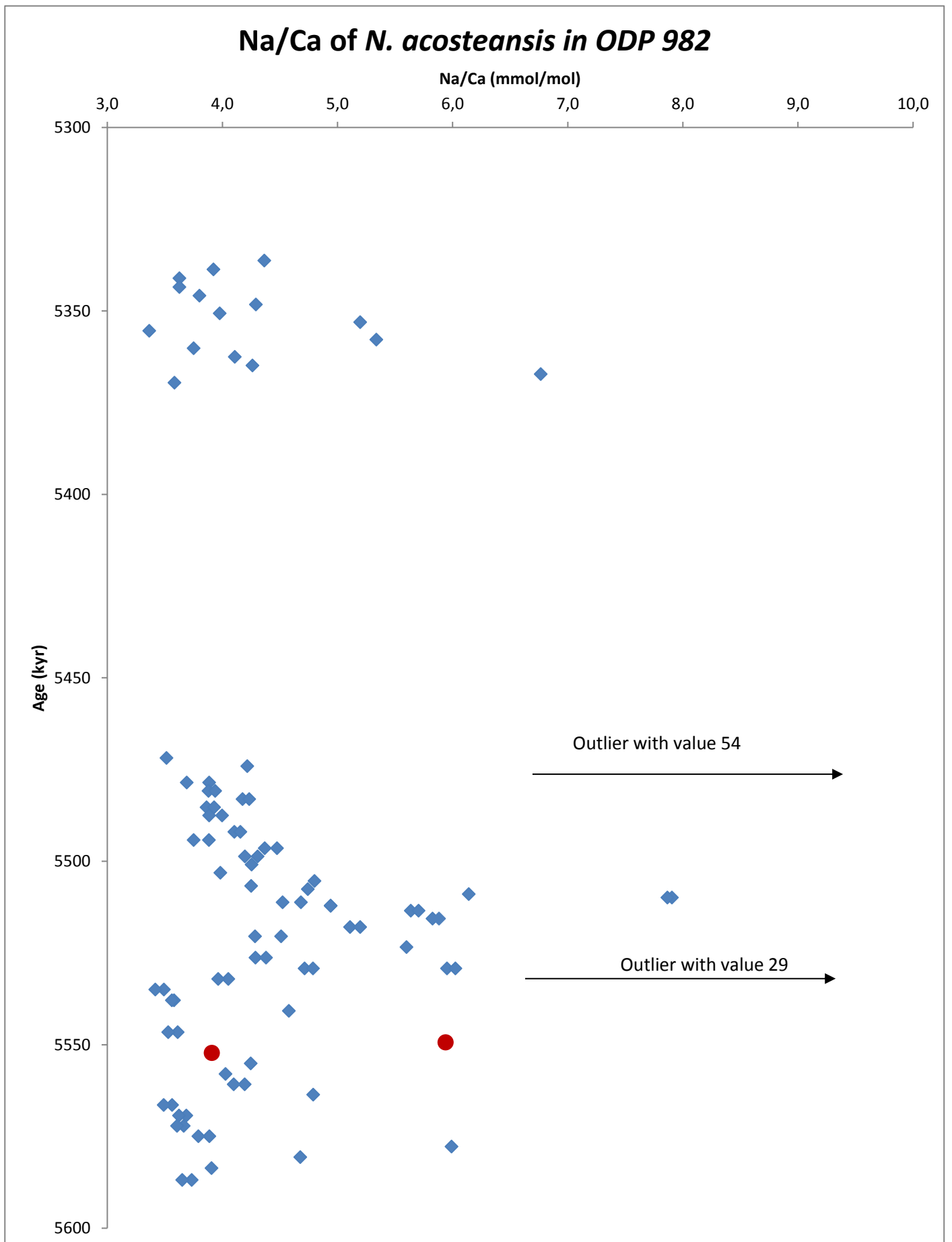
Figure 11. *The Na/Ca record measured in N. acostaensis from ODP core 982. The arrows indicate two outliers with highly aberrant values, that were probable erroneous. The two red circles indicate two samples where dextral N. acostaensis were used, because these samples were nearly devoid of sinistral specimens. These values were corrected for a species effect.*
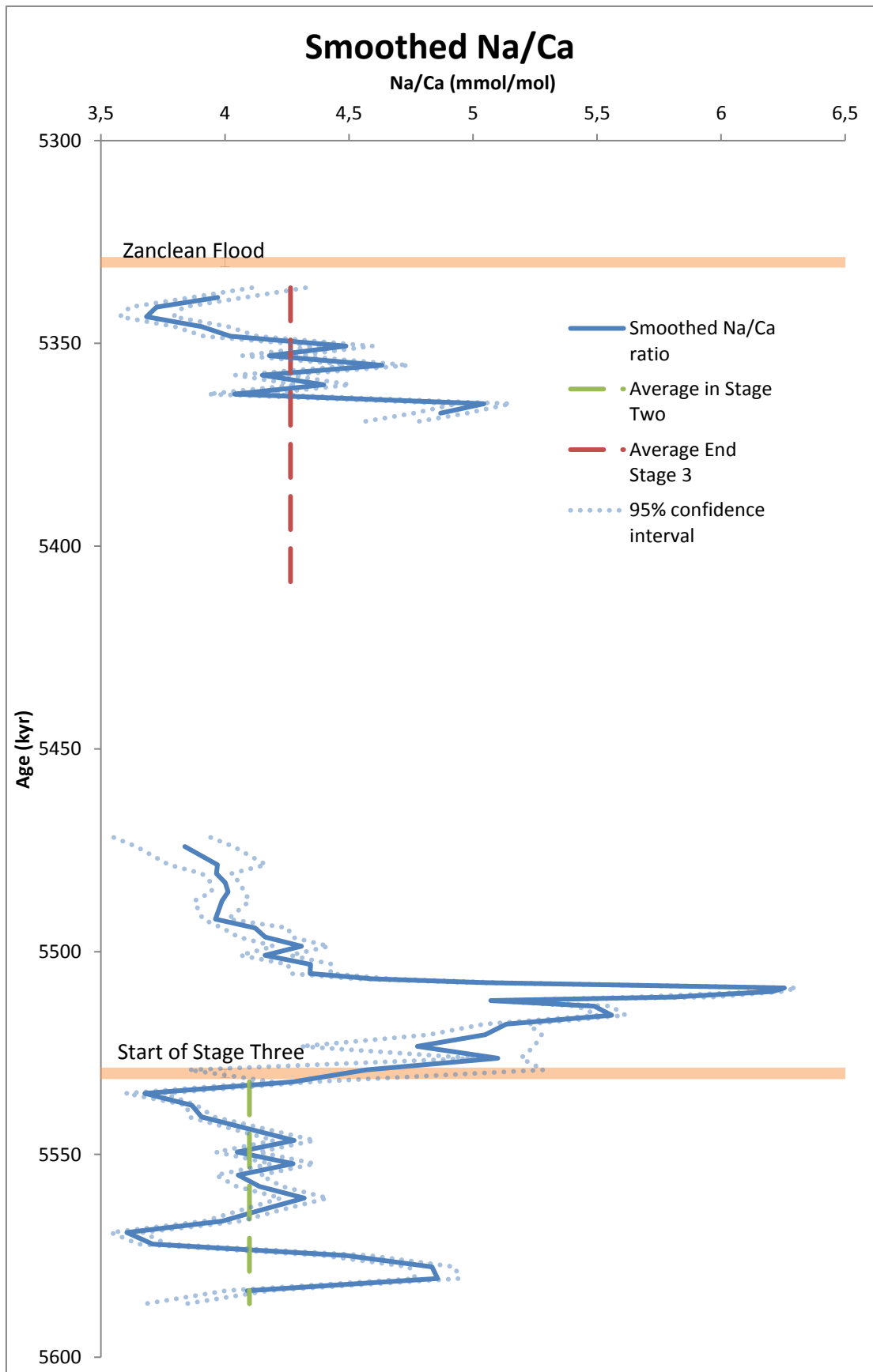
Figure 12. *The smoothed Na/Ca record is shown, with the confidence interval for the measurement. The orange lines indicate the start of Stage three of the MSC and the termination of the MSC in the Zanclean flood. The mean Na/Ca before and after stage three are shown to give an indication of the relative change.*
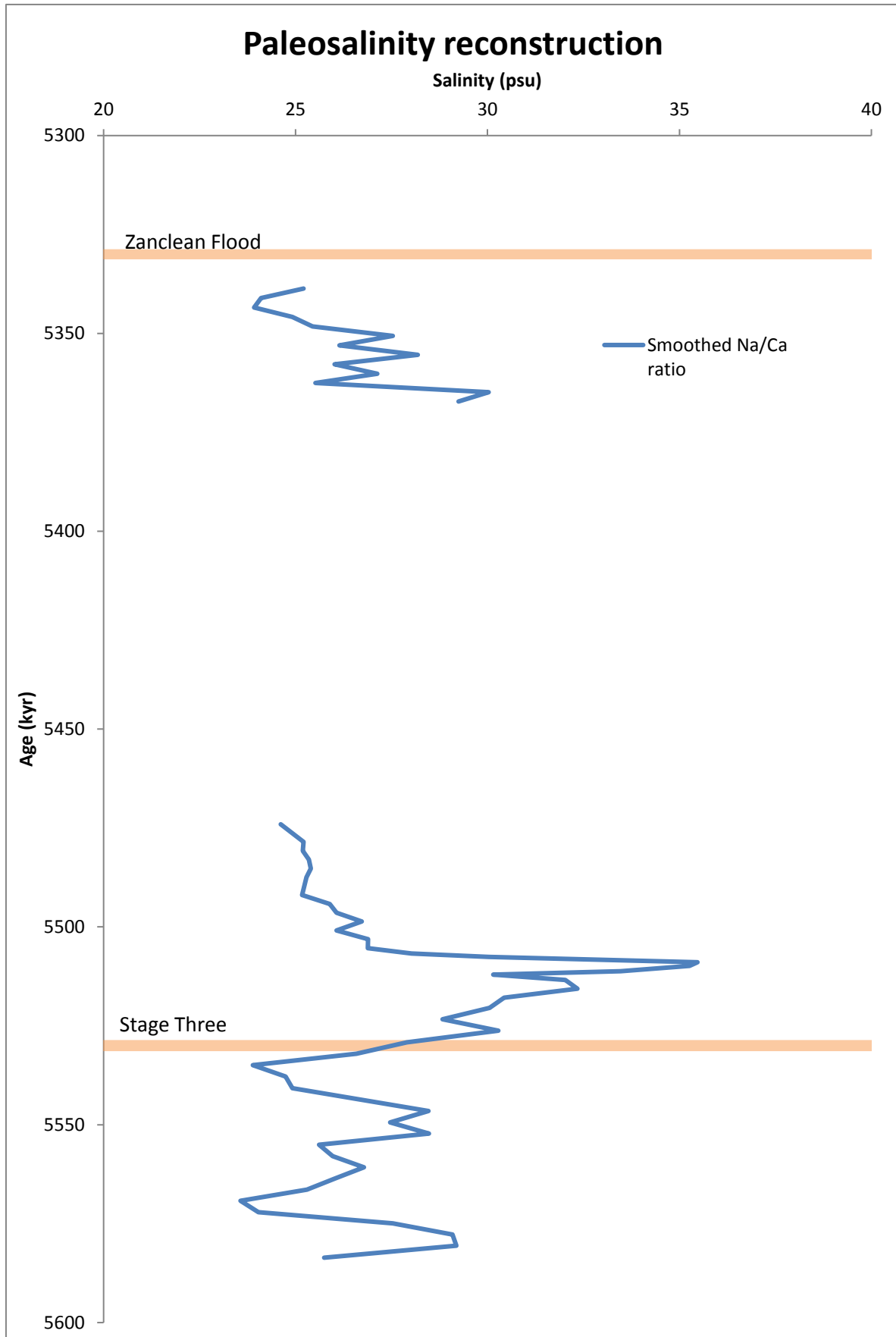
28

Figure 13. *A paleosalinity reconstruction based on the Na/Ca record of ODP 982 and the calibration based on the directional coefficient as measured in A. Tepida by Wit et al. (2013). The orange lines indicate the onset of stage three of the MSC and the termination of the MSC by the Zanclean Flood.*

6. Discussion

The research question of this study is: How can a North Atlantic marine record of paleosalinity give time constraints for the Mediterranean deep-basin setting during the MSC?

The current study investigated two hypotheses: 1) the paleosalinity reconstructed for the North Atlantic will show a decline over the course of the MSC, and 2) the rate of salinity decline was greater over stage 2 of the MSC than in either of the other stages. The first hypothesis has been falsified. The rate of decline is about equal in stages two and three. The only marked difference between the two stages is that there is a large pulse of Na/Ca in stage three. If this means anything then it is an indication of salinity increase in the North Atlantic, not a decrease.

The second hypothesis can also be rejected, the average Na/Ca, which is used as a proxy for salinity, is nearly the same at beginning and end of the studied interval. There is great variation in the record, but the mean value of the first and last 15 data points is nearly the same. No decline, or even a shift in salinity was detected in the North Atlantic over the MSC. Thus, this study revealed that the reconstructed paleosalinity record is not related events in the Mediterranean basin during the MSC. Therefore, the paleosalinity reconstruction does not give any time constraints for the MSC.

6.1 Data reliability

The Na/Ca data is likely to be rich in noise. Chemical instability of Na^+ in the calcite lattice of the foraminiferal tests (Evans et al. 2015) and influence of post depositional overgrowth (pers. com E. Geerken 2016) are vectors that could have introduced this noise. The tri-fold measurement of the younger interval shows that the Pearson correlation index between the two species of *N. acostaensis* is 0.49. This indicates that half of the variability between these two species is independent. Much of the independent variation is likely due to noise. Similar post depositional processes could have introduced correlated variability for the two species of *N. acostaensis*, thus the noise content of the Na/Ca record may have been even greater before the post depositional processes. The correlation between *N. acostaensis* and *N. atlantica* is much lower than the correlation between the two *N. acostaensis* species. This may be due to greater differences in species specific factors, or due to a different reaction to post depositional processes. All correlations based on Mg/Ca values are ca. 0.35 higher than the correlations based on Na/Ca with the same pairings. Thus 35% of the variability of the Na/Ca record may be due to random factors. Together this means that much of the variability of the Na/Ca record is noise, not a signal of salinity changes. There is still a component of the signal that may be preserved, but it is far from certain if it could be detected.

The maximum shift in salinity due to the MSC on the open ocean is ca. 5%, thus the reconstruction must be sensitive enough to detect a 5% decline in salinity to work. To detect salinity shifts over the stages of the MSC, even greater sensitivity to salinity is required. Due to the high noise content of the Na/Ca record, it is very likely that the record is not sensitive enough to make this detection.

Calibration of salinity to Na/Ca adds to the issues with reliability. The data from cruise 64PE275 make for a negative correlation between salinity and Na/Ca i.e. higher salinity leads to lower $[Na^+]$. This is opposite of what is found in other published data for calcite (Wit et al.,2013; Okumura &

Kitano, 1986). It also seems counterintuitive that the rate of Na+ incorporation declines as availability increases. It may be that the relationship between Na/Ca and salinity in *N. acostaensis* is of a more complex nature, such as a second or third power polynomial. Yet the negative linear calibration is the only one that is supported by the measurements. The calibration which is based on the correlation found by Wit et al. (2013) gives an unrealistically large range of salinities, from 25 to 35 psu, these values are considerably greater than the range observed today in the modern ocean. Due to the variability in the Na/Ca record, variations of 5 psu over 10 kyr are common. On this basis the calibration based on Wit et al. (2013) for *A. Tepida* can be rejected for *N. acostaensis*. The range of salinity values is much reduced if the calibration based on the data from 64PE275 is used, which makes them appear more credible, if chemically unlikely. Thus there remains much uncertainty about the magnitude and the direction of salinity shifts indicated by the Na/Ca record. Because the mean values of Na/Ca are nearly the same at the end, no salinity shift is detected. Therefore the hypotheses can be rejected even without knowledge about the direction or magnitude of salinity changes that correspond to shifts in Na/Ca.

6.2 The event at the onset of stage 3

The investigated records showed that the Na/Ca strongly increases at the start of stage 3 (5.53 Ma). Over 25 kyr the Na/Ca rises to the highest value in the record, then falls back down to some of the lowest values in the whole record over an 18 kyr interval. Stage 3 is present in the interpretation of the MSC by Roveri et al (2014) as well as in the deep basin Mediterranean record by Meijer et al. (2017). In stage 3 there were brackish water conditions in the Mediterranean area. Thus stage 3 may have had some influence on the halite budget of the open ocean and this peak around the onset of stage three looks interesting.

If an increase in Na/Ca is assumed to correlate to an increase in salinity, then the salinity at ODP 982 rose for 25 kyr around the onset of stage three and then in 18 kyr it fell back to the levels previously observed. A salinity increase over such a short interval would have been controlled by fluxes of salt due to erosion of salt deposits. The most likely area for this erosion seems to be the Mediterranean basin, where a shift to brackish waters could have led to the dissolution of deposited evaporites. Though currently there are no erosive surfaces that are currently with the onset of stage 3. If this pulse were to be linked to the erosive surface of stage 2, then it should be dated 5,5 Ma, not 5.6 Ma as is currently thought.

To raise salinities in the North Atlantic Ocean with dissolved evaporates from the Mediterranean basin the salt must have reached the North Atlantic Ocean through a gateway. Mediterranean outflow waters are bottom waters today, and a high saline water body would have had a high density, therefore any Mediterranean outflow water in the MSC is likely to have been a bottom water too. Any sill that caused gateway restriction would have severely reduced outflow before it could influence the inflow. Therefore a sustained outflow of high saline waters must have involved an opening and deepening of the gateway. This is in contradiction to the reduced influence of Atlantic waters detected by Flecker et al. (2015).

The high salinity pulse's transitory nature raises another question. If the rise of Na/Ca indicates transport of salts to the North Atlantic Ocean, then the subsequent fall requires that these salts were removed again. The only large scale sink for oceanic salts in the MSC, is the Mediterranean basin. Thus

the high Na/Ca a pulse would represent two Mediterranean milieus, first conditions which could mobilize large volumes of precipitated salts, then a shift back to precipitory conditions with salt deposition at a higher rate than the previous dissolution. Within the Mediterranean basin, traces of such a high variable system have not been found at the onset of stage 3. There is an erosive surface at the base of stage 2, but to link it to this pulse, the age model must be adjusted.

        Another possible explanation for the observed pulse is that the observed high salinities were not an ocean wide phenomenon, but instead only occurred locally in the area around ODP core 982. If high saline Mediterranean outflow water reached waters around ODP site 982, then mixing with the rest of the oceanic water could have removed the salt from the surface of the North Atlantic Ocean, but currently the Mediterranean outflow water does not flow towards the surface waters of the North Atlantic and it is not clear why this would have been different in the Miocene.

        $\Delta^{18}O$ and Mg/Ca are known to be influenced by salinity. Neither of these two records show a large shift around the high Na/Ca pulse at the start of stage three. While this is not impossible that proxies are influenced by other factors such as temperature and land ice volume to cancel out the reaction to the salinity shift, it does not seem likely that this happened for both proxies at the same time. The observed variation is also much lower in these two records, which shows that they were either less sensitive to the salinity swings indicated by the Na/Ca record, or that there was no large-scale salinity variation.

        Together this means that the high Na/Ca pulse is without a clear source of the salt to be exported, it involves unclear means of transportation to move this salt to the North Atlantic Ocean, and how this salt was then rapidly removed again are also unknown. If the relationship between Na/Ca and salinity is opposite, such a peak in Na/Ca indicates a trough in salinity, then the similar questions remain if in a different order. First a mass of evaporite must have been deposited in 25 kyr and then a similar volume must have been eroded in 18 kyr and the evaporite transported back to the North Atlantic Ocean.

        There is a possibility that the pulse is only random noise, but the variation in Na/Ca is nearly twice as great as the rest of the variation and it coincides closely to the onset of stage 3. This would make for a great coincidence. It might prove to be more fruitful to see the high Na/Ca pulse as a sign of an undefined event due to the onset of stage 3 in the Mediterranean basin, but to refrain from linking it solely to paleosalinity. This event at the onset of stage three is a question for further research. Detection of a similar event in the same interval in another record would confirm its observation. With that, it may yet prove possible to link the marine record from the North Atlantic to the Mediterranean region.

7. Conclusion

In this study a paleosalinity reconstruction was attempted based Na/Ca as a proxy salinity. This was done to link the marine record of a site in the North Atlantic to the deep basin setting of the Mediterranean during the MSC. This reconstruction seems to have been unreliable due to the poor preservation of the Na^+ signal in the calcite lattice. In the interval of the study where the same section was measured in three different species, the correlation between the three Na/Ca records was low, but for Mg/Ca and d18O the correlation was much higher. Thus it seems likely that the problems were specific to Na/Ca and its preservation, not the samples or the analysis.

Still no categorical change in the Na/Ca record could be detected over the latter two stages of the Messinian salinity crisis. There is no evidence to support the idea of rapid salt deposition in the Mediterranean basin. While it remains an interesting idea to link the events in the Mediterranean to those of the rest of the world's oceans, the apparent poor preservation of Na/Ca makes it ill-suited to this task in further research into paleosalinity. If further attempts at paleosalinity reconstruction are pursued, then another proxy should be used.

There is an event in the Na/Ca record of ODP982 around the onset of stage 3 of the MSC, which may prove of interest. If it can be linked to events in the Mediterranean basin then it may serve as a time constraint. It would then also be an indication that the onset of stage 3 had an influence of the marine chemistry of the North Atlantic Ocean, even if that influence may not have been on salinity. Without corroboration by another detection, or a credible mechanism to carry the signal from the Mediterranean to ODP site 982, the meaning of this high Na/Ca pulse remains an open question.

References

Agustí, J., M. Garcés and W. Krijgsman. 2006. "Evidence for African–Iberian Exchanges during the Messinian in the Spanish Mammalian Record." *Palaeogeography, Palaeoclimatology, Palaeoecology* 238(1):5-14.

Aze, T., T.H. Ezard, A. Purvis, H.K. Coxall, D.R. Stewart, B.S. Wade and P.N. Pearson. 2011. "A Phylogeny of Cenozoic Macroperforate Planktonic Foraminifera from Fossil Data." *Biological Reviews* 86(4):900-927.

Barker, S., M. Greaves and H. Elderfield. 2003. "A Study of Cleaning Procedures used for Foraminiferal Mg/Ca Paleothermometry." *Geochemistry, Geophysics, Geosystems* 4(9).

Baumann,K. and R. Huber. 1999. "12. Sea-Surface Gradients between the North Atlantic and the Norwegian Sea during the Last 3.1 My: Comparison of Sites 982 and 9851." 162:179.

Berggren, W.A. 1972. "A Cenozoic time-scale—some Implications for Regional Geology and Paleobiogeography." *Lethaia* 5(2):195-215.

Berner, Elizabeth K. and Robert A. Berner. 1987. *Global Water Cycle: Geochemistry and Environment.*Prentice-Hall.

Blanc-Valleron, M., C. Pierre, J. Caulet, A. Caruso, J. Rouchy, G. Cespuglio, R. Sprovieri, S. Pestrea and E. Di Stefano. 2002. "Sedimentary, Stable Isotope and Micropaleontological Records of Paleoceanographic Change in the Messinian Tripoli Formation (Sicily, Italy)." *Palaeogeography, Palaeoclimatology, Palaeoecology* 185(3):255-286.

Chester, Roy. 2009. *Marine Geochemistry.*John Wiley & Sons.

Cosentino, D., R. Buchwaldt, G. Sampalmieri, A. Iadanza, P. Cipollari, T.F. Schildgen, L.A. Hinnov, J. Ramezani and S.A. Bowring. 2013. "Refining the Mediterranean "Messinian Gap" with High-Precision U-Pb Zircon Geochronology, Central and Northern Italy." *Geology* 41(3):323-326.

Darling, K.F., M. Kucera, D. Kroon and C.M. Wade. 2006. "A Resolution for the Coiling Direction Paradox in Neogloboquadrina Pachyderma." *Paleoceanography* 21(2).

de Lange, G.J. and W. Krijgsman. 2010. "Messinian Salinity Crisis: A Novel Unifying Shallow gypsum/deep Dolomite Formation Mechanism." *Marine Geology* 275(1):273-277.

Duggen, S., K. Hoernle, P. van den Bogaard and C. Harris. 2004. "Magmatic Evolution of the Alboran Region: The Role of Subduction in Forming the Western Mediterranean and Causing the Messinian Salinity Crisis." *Earth and Planetary Science Letters* 218(1):91-108.

Duggen, S., K. Hoernle, P. Van Den Bogaard, L. Rüpke and J.P. Morgan. 2003. "Deep Roots of the Messinian Salinity Crisis." *Nature* 422(6932):602-606.

Eynaud, F., T. Cronin, S. Smith, S. Zaragosi, J. Mavel, Y. Mary, V. Mas and C. Pujol. 2009. "Morphological Variability of the Planktonic Foraminifer Neogloboquadrina Pachyderma from ACEX Cores: Implications for Late Pleistocene Circulation in the Arctic Ocean." *Micropaleontology*:101-116.

Ferguson, J., G. Henderson, M. Kucera and R. Rickaby. 2008. "Systematic Change of Foraminiferal Mg/Ca Ratios Across a Strong Salinity Gradient." *Earth and Planetary Science Letters* 265(1):153-166.

Flecker, R., W. Krijgsman, W. Capella, C. de Castro Martíns, E. Dmitrieva, J.P. Mayser, A. Marzocchi, S. Modestu, D. Ochoa and D. Simon. 2015. "Evolution of the Late Miocene Mediterranean–Atlantic Gateways and their Impact on Regional and Global Environmental Change." *Earth-Science Reviews* 150:365-392.

García-Alix, A., R. Minwer-Barakat, E. Martín Suárez, M. Freudenthal, J. Aguirre and F. Kaya. 2016. "Updating the Europe–Africa Small Mammal Exchange during the Late Messinian." *Journal of Biogeography*.

Gibert, L., G.R. Scott, P. Montoya, F.J. Ruiz-Sánchez, J. Morales, L. Luque, J. Abella and M. Lería. 2013. "Evidence for an African-Iberian Mammal Dispersal during the Pre-Evaporitic Messinian." *Geology* 41(6):691-694.

Gladstone, R., R. Flecker, P. Valdes, D. Lunt and P. Markwick. 2007. "The Mediterranean Hydrologic Budget from a Late Miocene Global Climate Simulation." *Palaeogeography, Palaeoclimatology, Palaeoecology* 251(2):254-267.

Govers, R., P. Meijer and W. Krijgsman. 2009. "Regional Isostatic Response to Messinian Salinity Crisis Events." *Tectonophysics* 463(1):109-129.

Hilgen, F., W. Krijgsman, I. Raffi, E. Turco and W. Zachariasse. 2000. "Integrated Stratigraphy and Astronomical Calibration of the Serravallian/Tortonian Boundary Section at Monte Gibliscemi (Sicily, Italy)." *Marine Micropaleontology* 38(3):181-211.

Hilgen, F., K. Kuiper, W. Krijgsman, E. Snel and E. van der Laan. 2007. "Astronomical Tuning as the Basis for High Resolution Chronostratigraphy: The Intricate History of the Messinian Salinity Crisis." *Stratigraphy* 4(2-3):231-238.

Hilgen, F.J., H.A. Aziz, W. Krijgsman, C.G. Langereis, L.J. Lourens, J.E. Meulenkamp, I. Raffi, J. Steenbrink, E. Turco and N. Van Vugt. 1999. "Present Status of the Astronomical (Polarity) Time-Scale for the Mediterranean Late Neogene." *Philosophical Transactions of the Royal Society of London A: Mathematical, Physical and Engineering Sciences* 357(1757):1931-1947.

Hilgen, F.J. and W. Krijgsman. 1999. "Cyclostratigraphy and Astrochronology of the Tripoli Diatomite Formation (Pre-Evaporite Messinian, Sicily, Italy)." *Terra Nova-Oxford* 11(1):16-22.

Hodell, D.A., J.H. Curtis, F.J. Sierro and M.E. Raymo. 2001. "Correlation of Late Miocene to Early Pliocene Sequences between the Mediterranean and North Atlantic." *Paleoceanography* 16(2):164-178.

Hodell, D.A. and J.P. Kennett. 1986. "Late Miocene–early Pliocene Stratigraphy and Paleoceanography of the South Atlantic and Southwest Pacific Oceans: A Synthesis." *Paleoceanography* 1(3):285-311.

Iaccarino,S.M. and A. Bossio. 1999. "42. Paleoenvironment of Uppermost Messinian Sequences in the Western Mediterranean (Sites 974, 975, and 978).":529-541.

Jansen,E., M.E. Raymo and P. Blum. 1996. "1. Leg 162: New Frontiers on Past Climates." 162:5-20.

Kamikuri, S., H. Nishi and I. Motoyama. 2007. "Effects of Late Neogene Climatic Cooling on North Pacific Radiolarian Assemblages and Oceanographic Conditions." *Palaeogeography, Palaeoclimatology, Palaeoecology* 249(3):370-392.

Kay Berner, E. and R. Berner. 1987. "The Global Water Cycle: Geochemistry and Environment.".

Klein, Cornelis, Cornelius S. Hurlbut and James D. Dana. 1993. *Manual of Mineralogy.*Wiley.

Kouwenhoven, T., F. Hilgen and G. Van der Zwaan. 2003. "Late Tortonian–early Messinian Stepwise Disruption of the Mediterranean–Atlantic Connections: Constraints from Benthic Foraminiferal and Geochemical Data." *Palaeogeography, Palaeoclimatology, Palaeoecology* 198(3):303-319.

Krijgsman, W., M. Blanc-Valleron, R. Flecker, F. Hilgen, T. Kouwenhoven, D. Merle, F. Orszag-Sperber and J. Rouchy. 2002. "The Onset of the Messinian Salinity Crisis in the Eastern Mediterranean (Pissouri Basin, Cyprus)." *Earth and Planetary Science Letters* 194(3):299-310.

Krijgsman, W., F. Hilgen, S. Marabini and G. Vai. 1999. "New Paleomagnetic and Cyclostratigraphic Age Constraints on the Messinian of the Northern Apennines (Vena Del Gesso Basin, Italy)." *Mem.Soc.Geol.it* 54:25-33.

Krijgsman, W. and P.T. Meijer. 2008. "Depositional Environments of the Mediterranean "Lower Evaporites" of the Messinian Salinity Crisis: Constraints from Quantitative Analyses." *Marine Geology* 253(3):73-81.

Krijgsman, W., M. Stoica, I. Vasiliev and V. Popov. 2010. "Rise and Fall of the Paratethys Sea during the Messinian Salinity Crisis." *Earth and Planetary Science Letters* 290(1):183-191.

Lewis, A.R., D.R. Marchant, A.C. Ashworth, L. Hedenas, S.R. Hemming, J.V. Johnson, M.J. Leng, M.L. Machlus, A.E. Newton, J.I. Raine, J.K. Willenbring, M. Williams and A.P. Wolfe. 2008. "Mid-Miocene Cooling and the Extinction of Tundra in Continental Antarctica." *Proceedings of the National Academy of Sciences of the United States of America* 105(31):10676-10680.

Lofi, J., F. Sage, J. Déverchère, L. Loncke, A. Maillard, V. Gaullier, I. Thinon, H. Gillet, P. Guennoc and C. Gorini. 2011. "Refining our Knowledge of the Messinian Salinity Crisis Records in the Offshore Domain through Multi-Site Seismic Analysis." *Bulletin De La Société Géologique De France* 182(2):163-180.

Lugli, S., M. Bassetti, V. Manzi, M. Barbieri, A. Longinelli and M. Roveri. 2007. "The Messinian 'Vena Del Gesso'evaporites Revisited: Characterization of Isotopic Composition and Organic Matter." *Geological Society, London, Special Publications* 285(1):179-190.

Manzi, V., R. Gennari, F. Hilgen, W. Krijgsman, S. Lugli, M. Roveri and F.J. Sierro. 2013. "Age Refinement of the Messinian Salinity Crisis Onset in the Mediterranean." *Terra Nova* 25(4):315-322.

Manzi, V., R. Gennari, S. Lugli, M. Roveri, N. Scafetta and B.C. Schreiber. 2012. "High-Frequency Cyclicity in the Mediterranean Messinian Evaporites: Evidence for solar–lunar Climate Forcing." *Journal of Sedimentary Research* 82(12):991-1005.

Manzi, V., S. Lugli, M. Roveri and B. Charlotte Schreiber. 2009. "A New Facies Model for the Upper Gypsum of Sicily (Italy): Chronological and Palaeoenvironmental Constraints for the Messinian Salinity Crisis in the Mediterranean." *Sedimentology* 56(7):1937-1960.

Marshak, S. 2011. Earth: Portrait of a Planet: Fourth International Student Edition.WW Norton & Company.

Meilijson,A., J. Steinberg, F. Hilgen, O. Bialik, P. Ilner, N. Waldmann and Y. Makovsky. 2017. "Integrated Stratigraphy and Chronology of Messinian Evaporites from the Levant Basin in the Deep Eastern Mediterranean." 19:5803.

Oddo, P., M. Adani, N. Pinardi, C. Fratianni, M. Tonani and D. Pettenuzzo. 2009. "A Nested Atlantic-Mediterranean Sea General Circulation Model for Operational Forecasting." *Ocean Science*.

Ohneiser, C., F. Florindo, P. Stocchi, A.P. Roberts, R.M. DeConto and D. Pollard. 2015. "Antarctic Glacio-Eustatic Contributions to Late Miocene Mediterranean Desiccation and Reflooding." *Nature Communications* 6.

Okumura, M. and Y. Kitano. 1986. "Coprecipitation of Alkali Metal Ions with Calcium Carbonate." *Geochimica Et Cosmochimica Acta* 50(1):49-58.

Poore, R. and W. Berggren. 1975. "Late Cenozoic Planktonic Foraminiferal Biostratigraphy and Paleoclimatology of Hatton-Rockall Basin; DSDP Site 116." *Journal of Foraminiferal Research* 5(4):270-293.

Riding, R., J.C. Braga and J.M. Martín. 1999. "Late Miocene Mediterranean Desiccation: Topography and Significance of theSalinity Crisis' Erosion Surface on-Land in Southeast Spain." *Sedimentary Geology* 123(1):1-7.

Riding, R., J.C. Braga, J.M. Martín and I.M. Sánchez-Almazo. 1998. "Mediterranean Messinian Salinity Crisis: Constraints from a Coeval Marginal Basin, Sorbas, Southeastern Spain." *Marine Geology* 146(1):1-20.

Roveri, M., A. Bertini, D. Cosentino, A. Di Stefano, R. Gennari, E. Gliozzi, F. Grossi, S.M. Iaccarino, S. Lugli and V. Manzi. 2008. "A High-Resolution Stratigraphic Framework for the Latest Messinian Events in the Mediterranean Area." *Stratigraphy* 5(3-4):323-342.

Roveri, M., R. Flecker, W. Krijgsman, J. Lofi, S. Lugli, V. Manzi, F.J. Sierro, A. Bertini, A. Camerlenghi and G. De Lange. 2014. "The Messinian Salinity Crisis: Past and Future of a Great Challenge for Marine Sciences." *Marine Geology* 352:25-58.

Ryan, W.B. 2009. "Decoding the Mediterranean Salinity Crisis." *Sedimentology* 56(1):95-136.

Ryan, W.B. 1976. "Quantitative Evaluation of the Depth of the Western Mediterranean before, during and After the Late Miocene Salinity Crisis." *Sedimentology* 23(6):791-813.

Selli, R., 1954. Il Bacino del Matauro. Giornale di Geologia 24, 1-294.

Selli, R., 1960 Il Messiniano Mayer-Eymar 1867. Proposta di un neostratotipo. Giornale di Geologia 28, 1-33.

Sierro, F., J. Flores, G. Francés, A. Vazquez, R. Utrilla, I. Zamarreño, H. Erlenkeuser and M. Barcena. 2003. "Orbitally-Controlled Oscillations in Planktic Communities and Cyclic Changes in Western Mediterranean Hydrography during the Messinian." *Palaeogeography, Palaeoclimatology, Palaeoecology* 190:289-316.

Soto-Navarro, J., F. Criado-Aldeanueva, J. García-Lafuente and A. Sánchez-Román. 2010. "Estimation of the Atlantic Inflow through the Strait of Gibraltar from Climatological and in Situ Data." *Journal of Geophysical Research: Oceans* 115(C10).

Tulbure, M., W. Capella, N. Barhoun, J. Flores, F. Hilgen, W. Krijgsman, T. Kouwenhoven, F. Sierro and M. Yousfi. 2017. "Age Refinement and Basin Evolution of the North Rifian Corridor (Morocco): No Evidence for a Marine Connection during the Messinian Salinity Crisis." *Palaeogeography, Palaeoclimatology, Palaeoecology*.

Ujiié, Y. and Y. Ishitani. 2016. "Evolution of a Planktonic Foraminifer during Environmental Changes in the Tropical Oceans." *PloS One* 11(2):e0148847.

Van Couvering, J.A., D. Castradori, M.B. Cita, F.J. Hilgen and D. Rio. 2000. "The Base of the Zanclean Stage and of the Pliocene Series." *Episodes* 23(3):179-187.

Vara, A., R.P. Topper, P.T. Meijer and T.J. Kouwenhoven. 2015. "Water Exchange through the Betic and Rifian Corridors Prior to the Messinian Salinity Crisis: A Model Study." *Paleoceanography* 30(5):548-557.

Vaughan, S., R. Bailey and D. Smith. 2011. "Detecting Cycles in Stratigraphic Data: Spectral Analysis in the Presence of Red Noise." *Paleoceanography* 26(4).

Warren, J.K. 2010. "Evaporites through Time: Tectonic, Climatic and Eustatic Controls in Marine and Nonmarine Deposits." *Earth-Science Reviews* 98(3):217-268.

Weaver, P.P. and B.M. Clement. 1986. "Synchroneity of Pliocene Planktonic Foraminiferal Datums in the North Atlantic." *Marine Micropaleontology* 10(4):295-307.

Wit, J.C., L. de Nooijer, M. Wolthers and G. Reichart. 2013. "A Novel Salinity Proxy Based on Na Incorporation into Foraminiferal Calcite." *Biogeosciences* 10(10):6375-6387.

Zachariasse,W. 1992. "Neogene Planktonic Foraminifers from Sites 761 and 762 Off Northwest Australia." 122:665-675.

Zachariasse, W., L. Gudjonsson, F. Hilgen, L. Lourens and P. Verhallen. 1990. "Late Gauss to Early Matuyama Invasions of Neogloboquadrina Atlantica in the Mediterranean and Associated Record of Climatic Change." *Astronomical Forcing of Mediterranean Climate during the Last 5.3 Million Years*:21.